Synchrotron Radiation Research Center

An overview of the magnet measurement development at SRRC

C. S. Hwang, T. C. Fan, F. Y. Lin

Synchrotron Radiation Research Center (SRRC),

Hsinchu, Taiwan

Outline

- Introduction
- 3-D moving with fixed angle Hall probe system
- Simple rotating coil system
- Flip and stretch wire system
- Three-orthogonal axes Hall probe system
- Highly automatic Helmholtz system
- Pulse-wire system

Introduction

Magnetic Field Measurement System

- Lattice magnet
  - Moving fixed angle Hall probe system => point-by-point
  - Rotating coil system => global measurement
  - Stretch wire system => simple mechanism
- Insertion device magnet
  - Three-orthogonal Hall probe system => helical field
  - Highly automatic Helmholtz system => magnet block
  - Pulse-wire system => mini-gap undulator
  - Stretch wire system => multipole shimming

3-D moving with fixed angle Hall probe system

❖ Advantages:

- **Point field and integral field**
- **Gradient field**
- **Static or or time-varying field**
- ***Large curvature bending magnet* or *combined function dipole magnet***
- ***Provide detail information* for the magnet shimming**
- ***higher precision harmonic field analysis***

❖ Disadvantage and crucial issues:

- Time consuming
- The long term stability is not so high
- Skew dipole component can not be found

Point field mapping with fixed angle Hall probe

- Operation principle of Hall probe

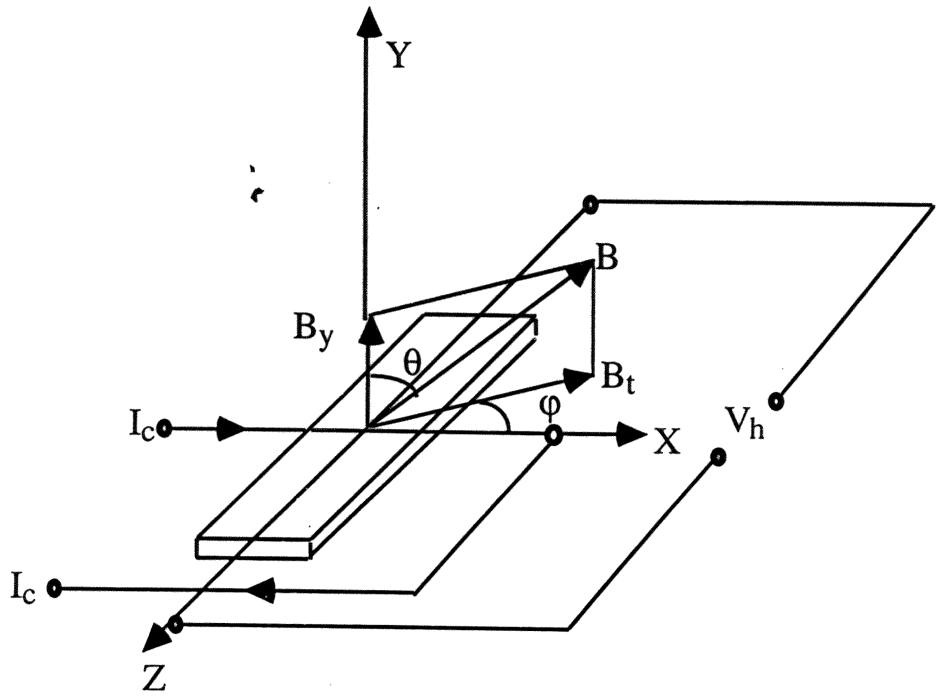

$$Vh = V0 + Rh\, By\, Ic - P\, Bt^2\, Ic\, \sin(2\varphi)$$

Where $Bt = Bo \sin\theta$, $By = Bo \cos\theta$, $P = K_2(\alpha_t - \alpha_l)$

$$\Delta B = (1/24)\, L^2 \left.\frac{d^2B(x)}{dx^2}\right|_{x=0} + (1/1920)\, L \left.\frac{d^4B(x)}{dx^4}\right|_{x=0} + \cdots\cdots$$

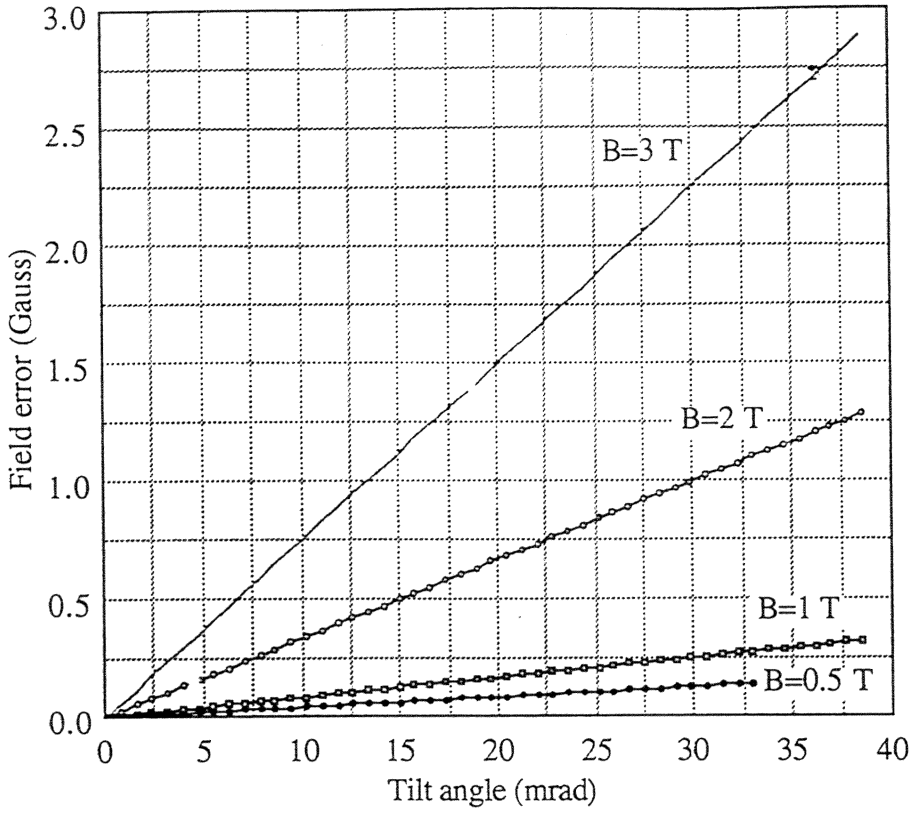

FIG. 2. The field error ΔB dependency on the different angle φ and transverse field B_t.

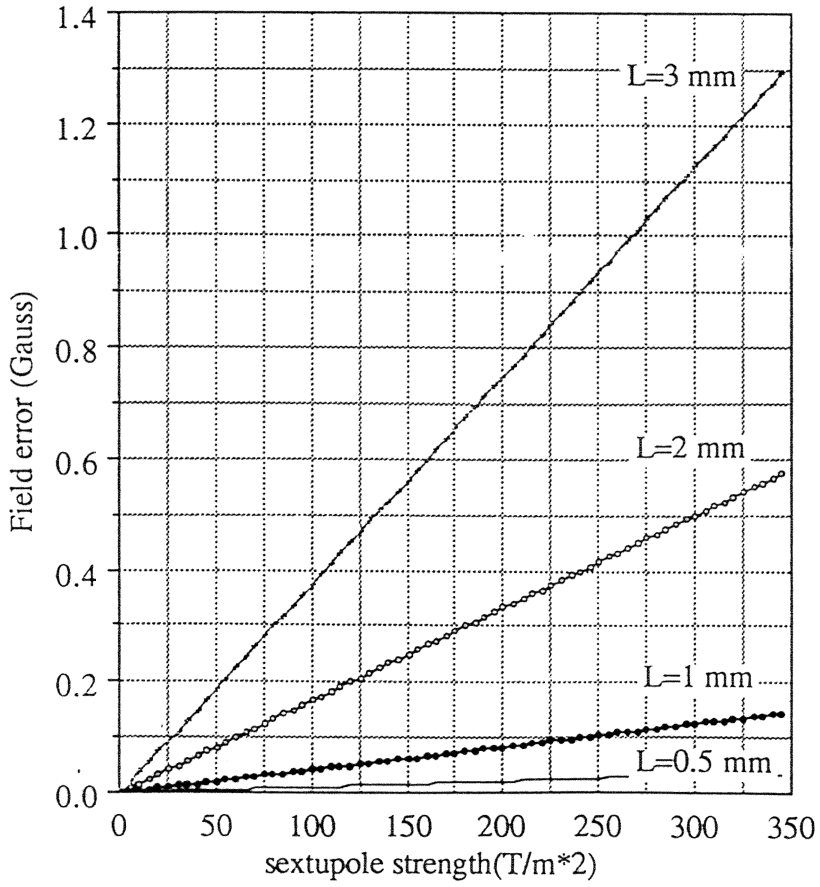

FIG. 3. The field error ΔB dependency on the different lengths of the Hall-probe sensitive area and sextupole strength of the magnet.

(a) Symmetry multipole magnet

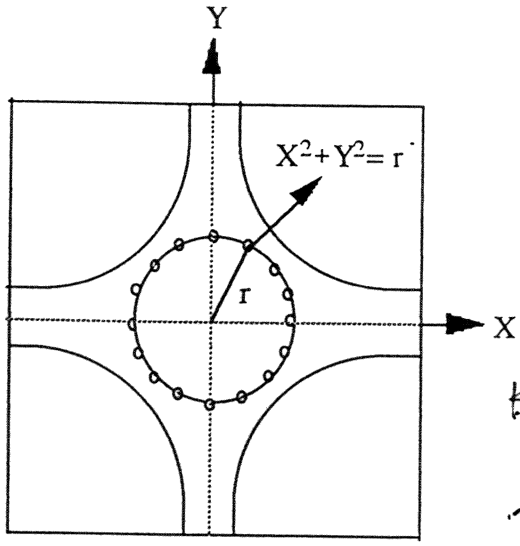

(b) Bending magnet

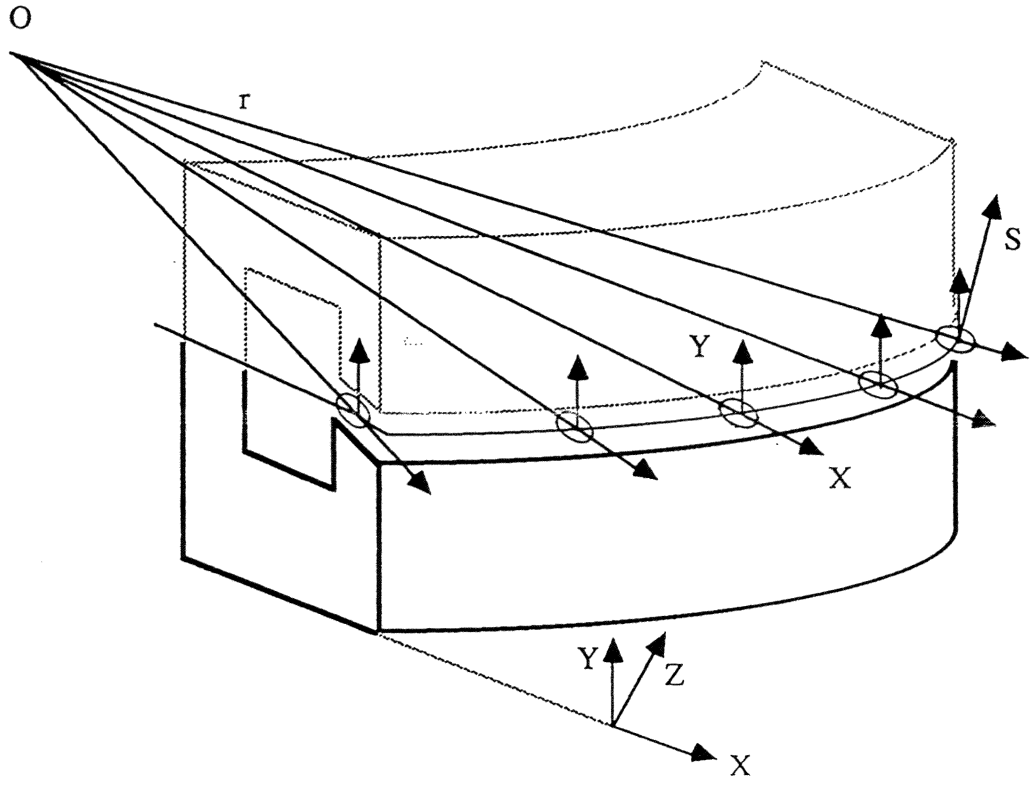

FIG. 2.2. (a) The circular mapping trajectory on the transverse plane of the symmetry pole magnet (e.g. quadrupole and sextupole magnets e.s.c), (b) The geometrical construction and ellipsoidal equation mapping trajectory on the transverse plane of the TBA dipole.

Harmonic field analysis method using Hall probe:

$$B_y(x,y,z) = \sum_{n=1}^{n}\sum_{m=0}^{m} N_{nm} H_n^N(z) x^{n-2m-1} y^{2m} + \sum_{n=2}^{n}\sum_{m=0}^{m} S_{nm} H_n^S(z) x^{n-2m-2} y^{2m+1}.$$

If the Hall probe is rotated 90° precisely, the $B_x(x,y,z)$ can be expressed as

$$B_x(x,y,z) = \sum_{n=1}^{n}\sum_{m=0}^{m} N_{nm} H_n^N(z) y^{n-2m-1} x^{2m} + \sum_{n=2}^{n}\sum_{m=0}^{m} S_{nm} H_n^S(z) y^{n-2m-2} x^{2m+1},$$

$$N_{nm} = (-1)^m\, n!/(n\text{-}2m)!(2m)!,$$

$$S_{nm} = (-1)^m\, n!/(n\text{-}2m\text{-}1)!(2m+1)!.$$

Where N_{nm} and S_{nm} are the weighting factors. Equation (2.7) would be used to fit the measurement data by the non-linear least square fitting method. The coefficients $H_n^N(z)$ and $H_n^S(z)$ represent the normal term and skew term,respectively. Therefore, the arbitrary orientation angle for the *nth* harmonic is equal to

$$\alpha_n(z) = \sin^{-1}(H_n^N(z)/H_n(z)),$$

and the total harmonic strength $H_n(z)$

$$B_y(r,\theta,z) = \sum_{n=1}^{n} H_n(z) r^{n-1}\{\sin(n\theta - \alpha_n(z))\},$$

Where θ is the phase angle and $\alpha_1(z)$ is the unknown. Since the Hall probe can be used to perform point by point mapping. The amplitude and the arbitrary orientation angle are dependent on z. To find the integrated values of $H_n(z)$ and $\alpha_n(z)$, an iteration through the individual points is made which is termed as the trapezoidal rule. So the integrated values are

$$\int_{-\infty}^{\infty} B_y(r,\theta,z)dz = \sum_{n=1}^{n} H_n r^{n-1}[\sin(n\theta - \alpha_n)],$$

$$\alpha_n = \sin^{-1}(H_n^N/H_n).$$

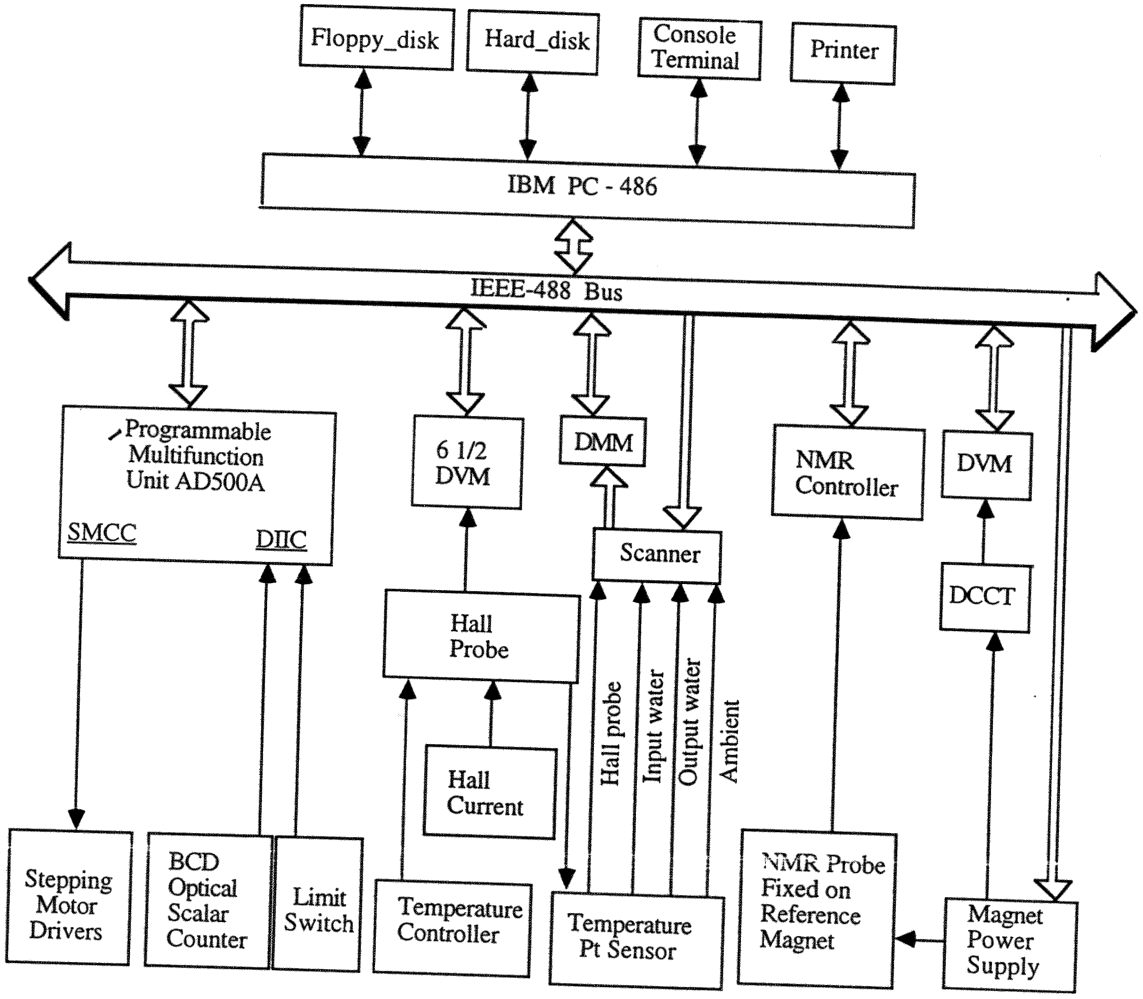

FIG. 2.3 Schematic functional block diagram of the hardware configuration for the real-time full-automatically magnetic field measurement system.

The harmonic field integrated strength comparison between the Hall probe methoc and the rotating harmonic coil method. For the quadrupole and sextupole field and normalized at a good field region location $x=\pm 0.03$ m, where $H_2(0)=12.7$ T/m for quadrupole magnet and $H_3(0) = 120$ T/m^2 sextupole magnet.

	Quadrupole					
	$(A_3)_2$ (%)	$(A_4)_2$ (%)	$(A_5)_2$ (%)	$(A_6)_2$ (%)	$(A_{10})_2$ (%)	$(A_{14})_2$ (%)
Hall probe	0.020	0.029	0.004	0.022	0.032	0.017
Rotating coil	0.025	0.023	0.005	0.015	0.029	0.013
	Sextupole					
	$(A_4)_3$ (%)	$(A_5)_3$ (%)	$(A_6)_3$ (%)	$(A_9)_3$ (%)	$(A_{15})_3$ (%)	
Hall probe	0.105	0.042	0.014	0.082	0.010	
Rotating coil	0.106	0.044	0.010	0.076	0.015	

The comparison between the two dimensional theoretica calculation and the mapping results by the Hall probe method for the dipole, quadrupole and sextupole magnet.

Magnet type	Harmonic Number n	Field strength (T/m^{n-1}) $H_n(0)$		Phase ($\alpha_n(0)$)	
		Theoretical	Measurement	Theoretical	Measurement
Dipole	1	1.24044	1.24044	--------	--------
	2	1.71075	1.71746	- 90°	-89.63°
	3	0.054	0.085	- 90°	-110.75°
	4	2.87	10.49	90°	75.29°
	5	74.86	264.1	- 90°	78.27°
	6	3.83×10^3	1.26×10^3	- 90°	-86.11°
	7	5.69×10^5	3.53×10^5	90°	97.85°
	9	4.48×10^9	7.95×10^8	- 90°	-83.95°
Quadrupole	1	0.0	3.97×10^{-6}	--------	--------
	2	12	12	90°	90.05°
	3	0.0	0.119	0°	164.25°
	4	0.8	5.39	90°	83.79°
	5	0.0	47.99	0°	45.23°
	6	5.21×10^3	6.87×10^3	90°	94.00°
	10	6.35×10^9	3.65×10^9	- 90°	-73.71°
	14	7.01×10^{15}	5.59×10^{15}	- 90°	-73.42°
Sextupole	1	3.41×10^{-4}	2.37×10^{-4}	--------	--------
	2	4.99×10^{-14}	0.0044	- 3.46°	-1.73°
	3	229.18	229.18	90°	89.94°
	4	9.11×10^{-10}	0.838	-45.71°	83.79°
	5	43.32	132.1	- 90°	72.35°
	6	1.82×10^{-6}	1.29×10^3	168.49°	79.67°
	9	2.56×10^8	2.04×10^8	90°	-91.35°
	15	2.20×10^{17}	4.50×10^{16}	90°	-115.65°

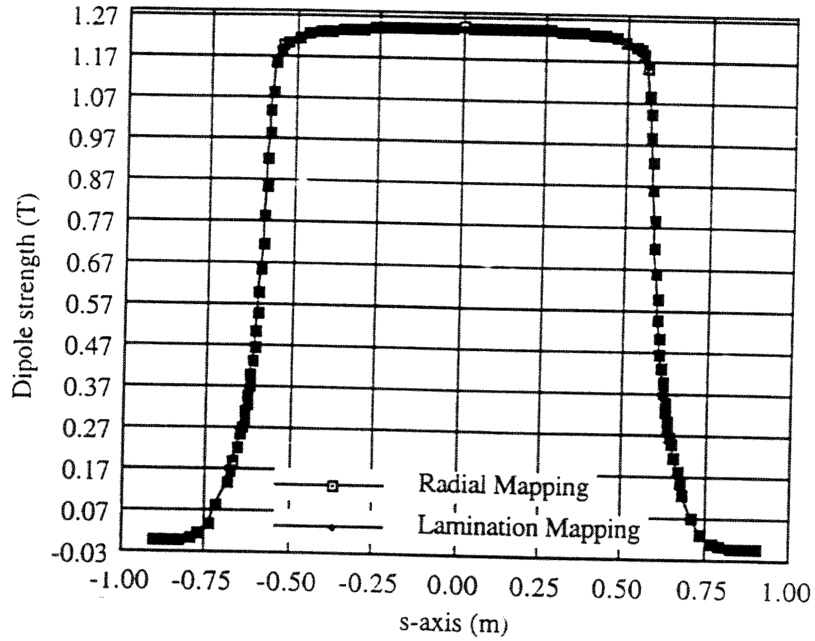

Fig. 2. Dipole field distribution along the longitudinal direction of the two mapping methods.

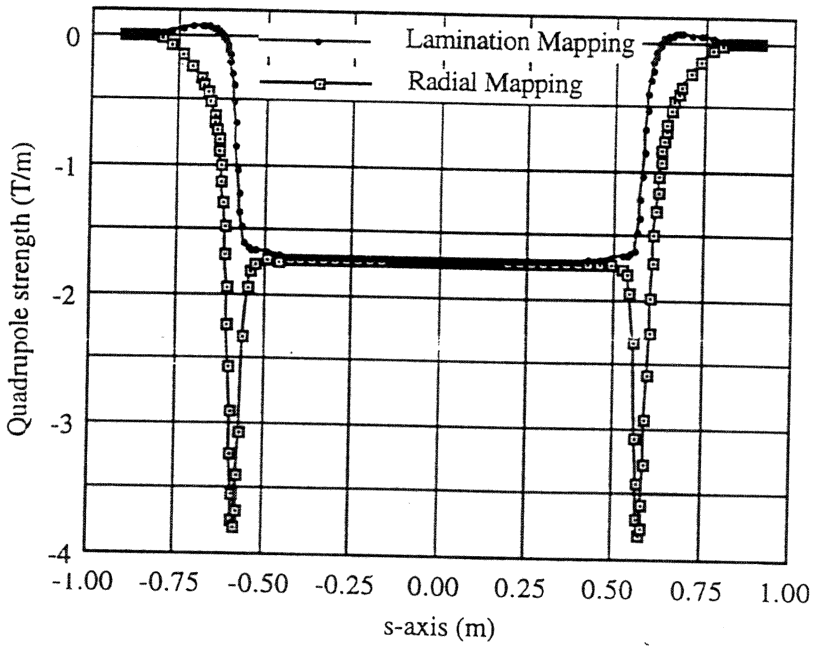

Fig. 3. Quadrupole field distribution along the longitudinal direction of the two mapping methods.

(a)

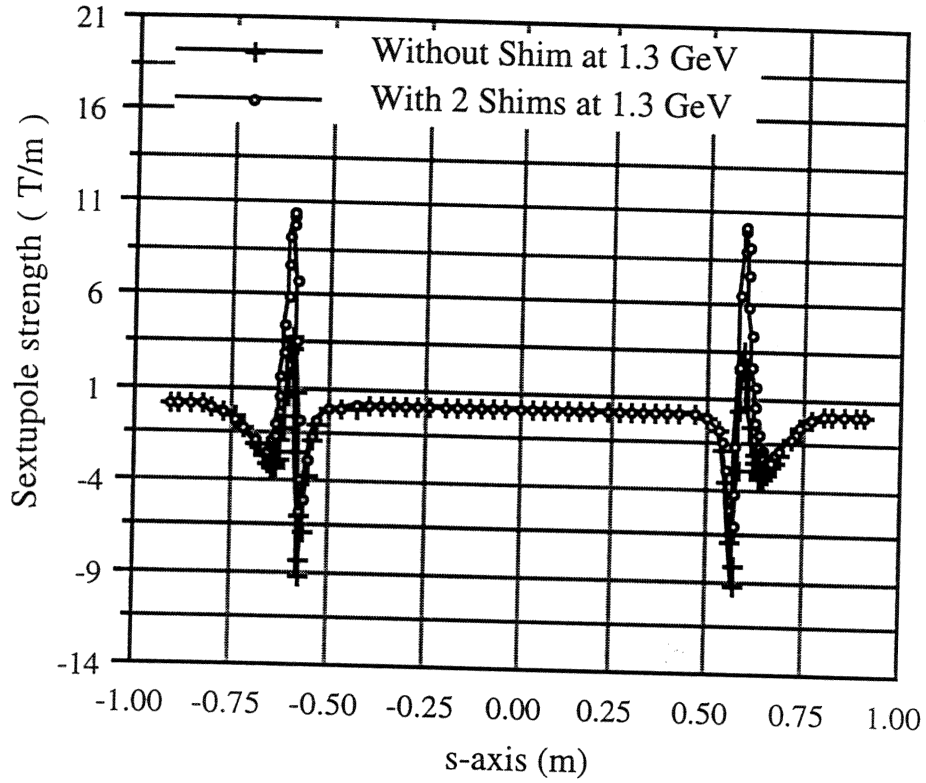

(b)

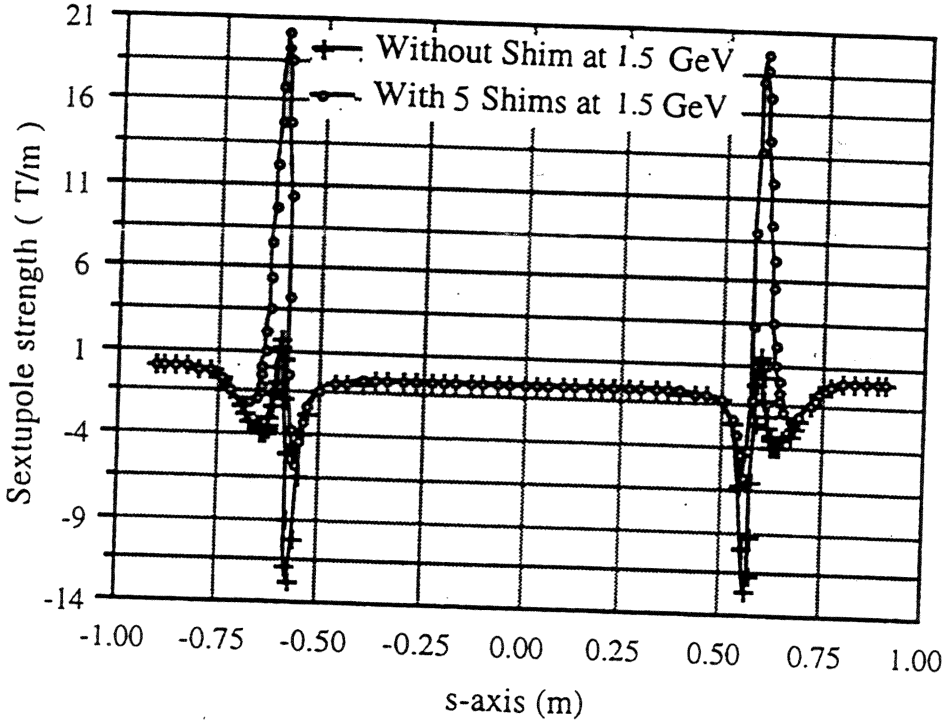

FIG. 4.4 Distribution of sextupole field strength along the longitudinal direction with and without shims at (a) 1.3 GeV and (b) 1.5 GeV.

Quadrupole magnet:

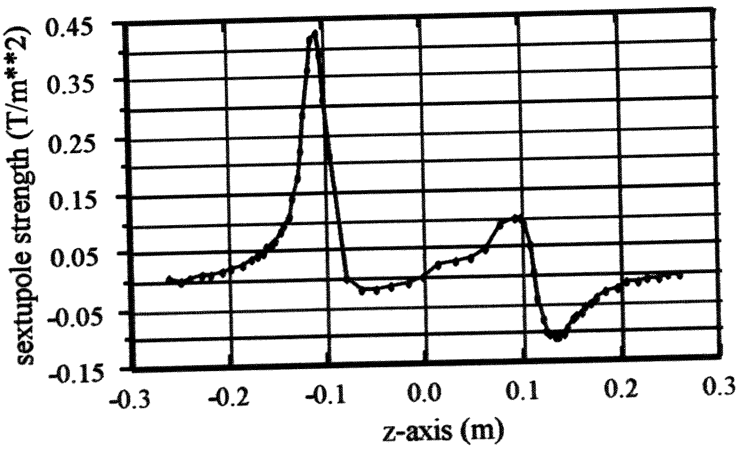

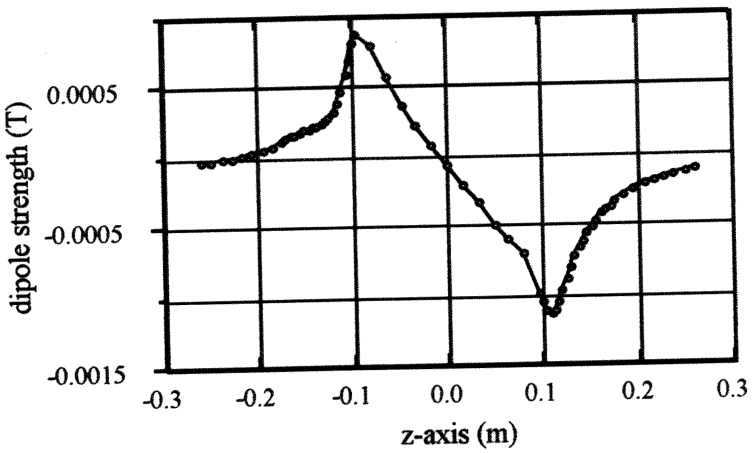

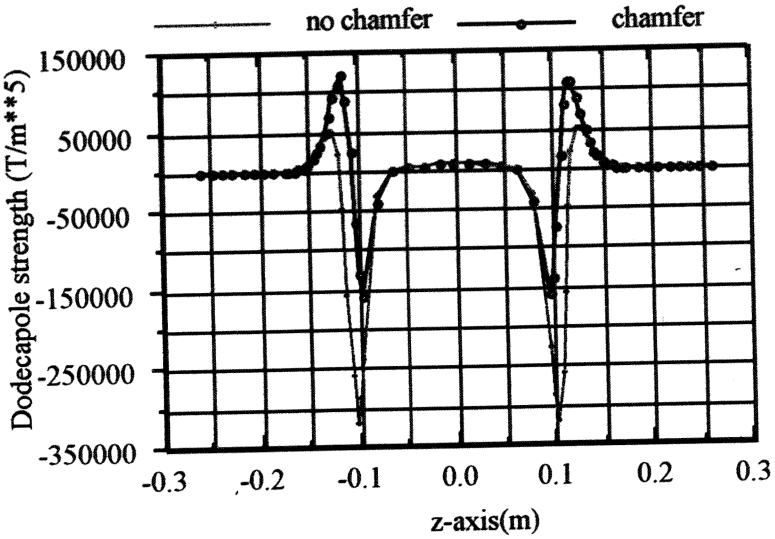

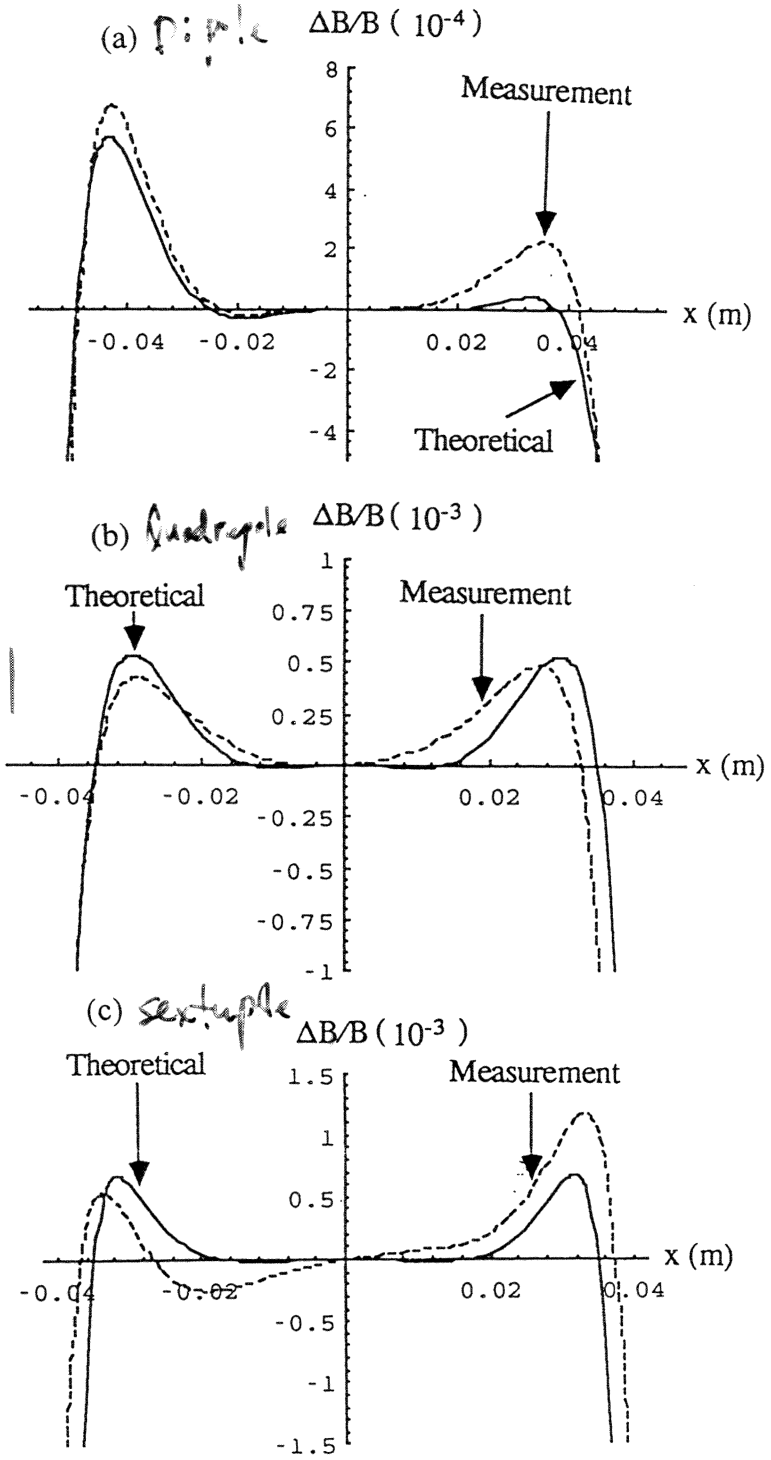

FIG. 2.4 The field deviation as a function of x of the two dimensional theoretical calculation, and the measurement results of (a) the combined function bending magnet, (b) the quadrupole magnet. Where the field deviation definition is $\Delta B_y/B_y = [B_y(x) - (H_1(0)+H_2(0)x)]/(H_1(0)+H_2(0)x)$, and (c) the sextupole magnet. Where the field deviation definition is $\Delta B_y/B_y = [B_y(x) - (H_1(0)+H_2(0)x+H_3(0)x^2)]/(H_1(0)+H_2(0)x+H_3(0)x^2)$.

(a)

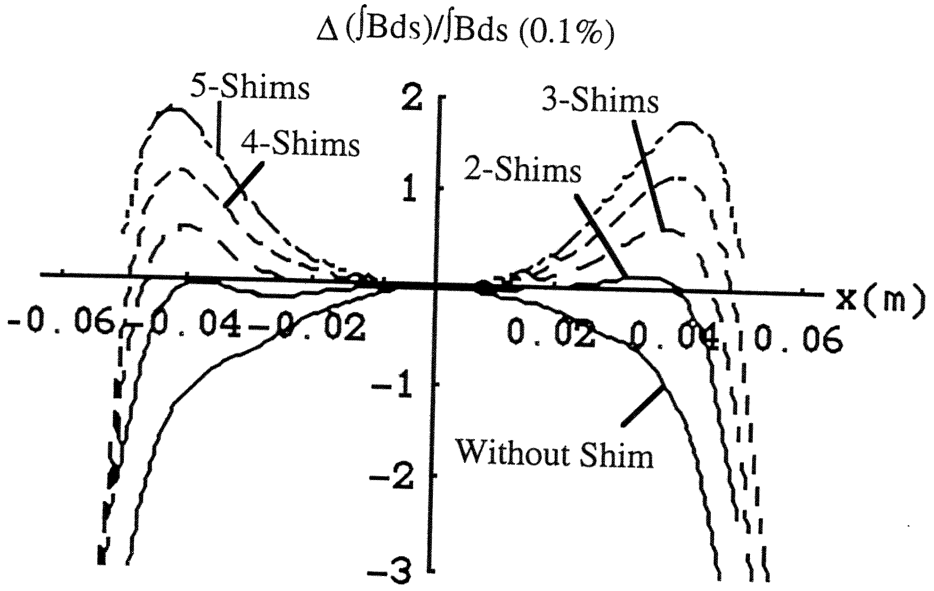

(b)

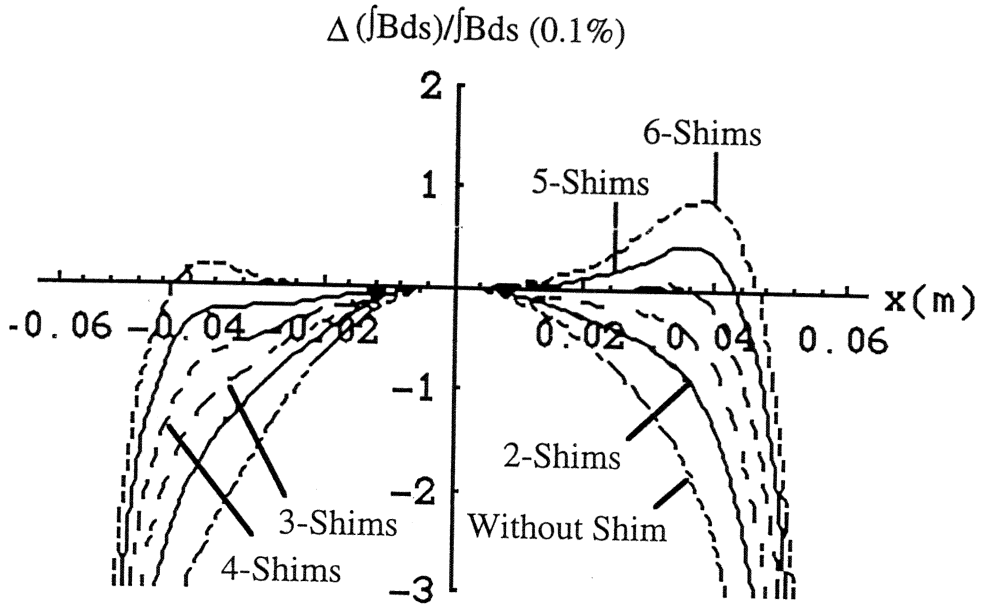

FIG. 4.3 Deviation of higher multipole integral strength ∫Bds with and without shims at the excitation current of (a) nominal excitation current 940 A (1.3 GeV) and (b) 1195 A (1.5 GeV).

(a)

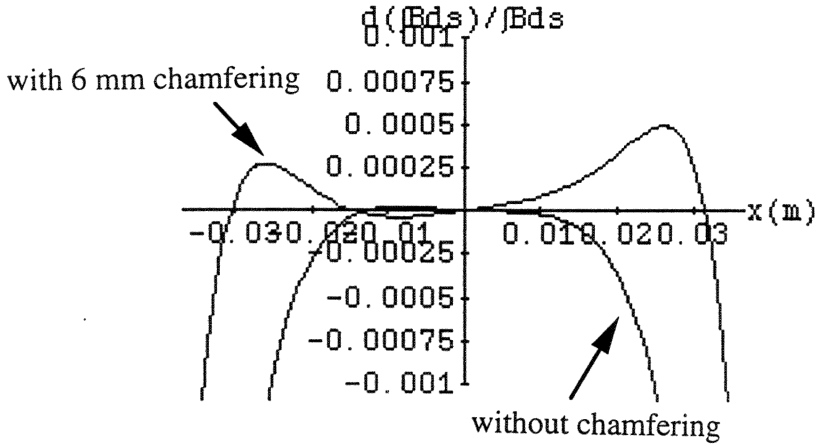

(b)

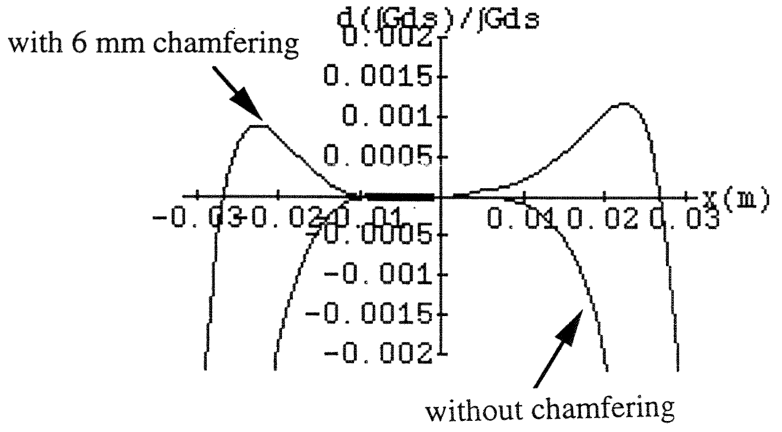

FIG. 4.8 (a) the integrated field deviation and (b) the integral gradient field deviation are as a function of transverse direction of the before and after chamfering results on the midplane.

Helmholtz coil method with 3-D rotation mechanism

❖ Advantages:

- It is highly automatic and high speed measurement system for reducing the human error and the time consuming
- The three *magnetic dipole moment components* can be obtained for once block installation
- *Fast speed measurement for 90 s/magnet*

❖ *crucial* issues:

- **It is a very complex system on the drive train mechanism**
- **We should pre-run the system before starting the field measurement**
- **Mechanical drive train system is not so reliable for a long time test**

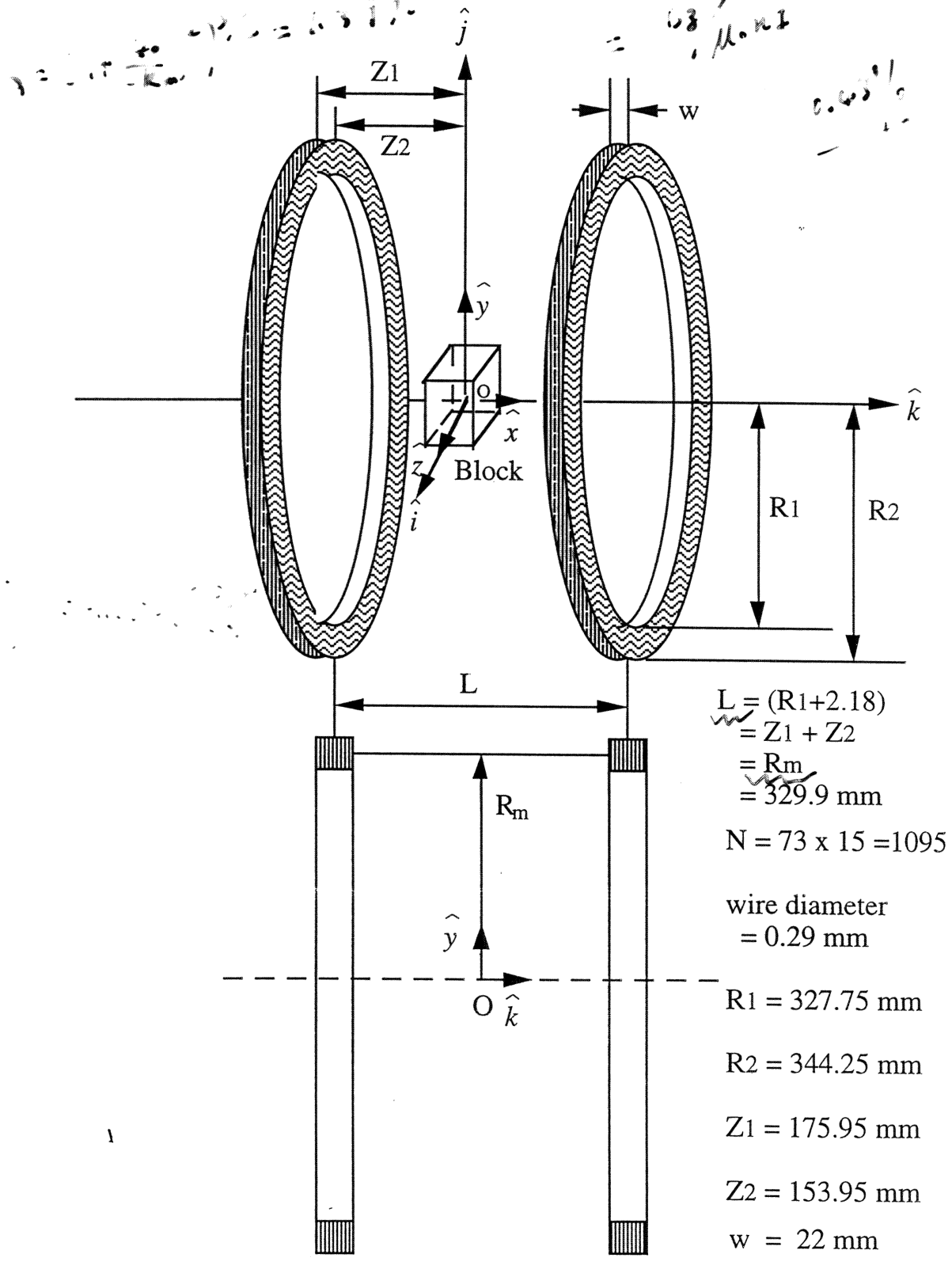

FIG. 3.9 The Helmholtz coil pair coordinate and its structure as well as the magnet coordinate system.

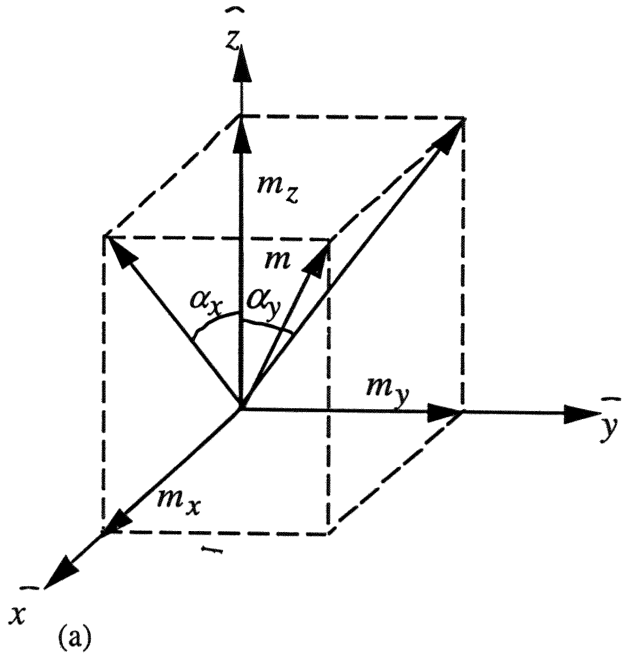

(a)

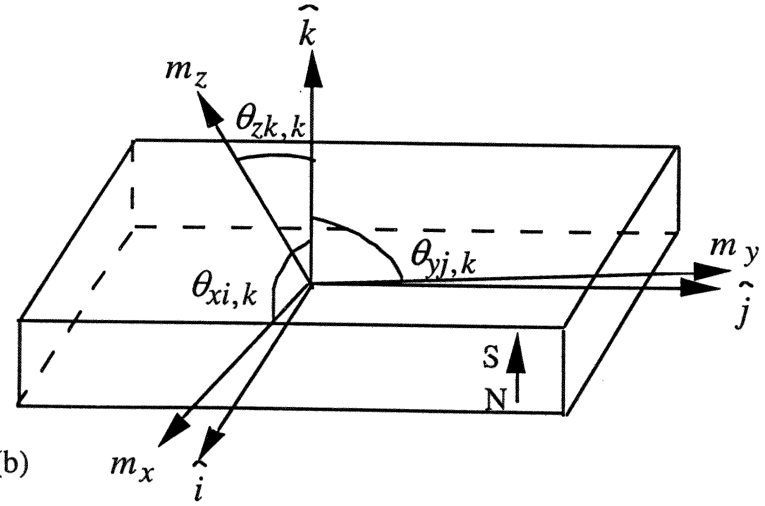

(b)

$$\vec{m} = m_x \hat{x} + m_y \hat{y} + m_z \hat{z} ,$$

$$m = \sqrt{m_x^2 + m_y^2 + m_z^2} ,$$

$$\alpha_x = tan^{-1}\left(\frac{m_x}{m_z}\right),$$

$$\alpha_y = tan^{-1}\left(\frac{m_y}{m_z}\right) .$$

$$M_k = \vec{m} \cdot \hat{k} = m_x \hat{x} \cdot \hat{k} + m_y \hat{y} \cdot \hat{k} + m_z \hat{z} \cdot \hat{k}$$

$$= m_x \cos \theta_{xi,k} + m_y \cos \theta_{yj,k} + m_z \cos \theta_{zk,k} ,$$

The first step consists of rotating the block holder by 360° around the $\hat{j}$-*axis* to obtain the magnetic flux linkage at the four angles of 0°, 90°, 180°, 270° :

$$\Psi_1 = K\,(m_x \cos\theta_{xk,k} + m_y \cos\theta_{yi,k} - m_z \cos\theta_{zj,k}),$$

$$\Psi_2 = K\,(m_x \cos\theta_{xi,k} - m_y \cos\theta_{yk,k} - m_z \cos\theta_{zj,k}),$$

$$\Psi_3 = K\,(-m_x \cos\theta_{xk,k} - m_y \cos\theta_{yi,k} - m_z \cos\theta_{zj,k}),$$

$$\Psi_4 = K\,(-m_x \cos\theta_{xi,k} + m_y \cos\theta_{yk,k} - m_z \cos\theta_{zj,k}).$$

Rotating the holder by a 180° rotation around the $\hat{k}$-*axis* and then again measuring the magnetic flux at four angles by a 360° rotation around the $\hat{j}$-*axis*:

$$\Psi_5 = K\,(m_x \cos\theta_{xk,k} - m_y \cos\theta_{yi,k} + m_z \cos\theta_{zj,k}),$$

$$\Psi_6 = K\,(m_x \cos\theta_{xi,k} + m_y \cos\theta_{yk,k} + m_z \cos\theta_{zj,k}),$$

$$\Psi_7 = K\,(-m_x \cos\theta_{xk,k} + m_y \cos\theta_{yi,k} + m_z \cos\theta_{zj,k}),$$

$$\Psi_8 = K\,(-m_x \cos\theta_{xi,k} - m_y \cos\theta_{yk,k} + m_z \cos\theta_{zj,k}).$$

The last step consists of rotating the block by 90° around the $\hat{i}$-*axis* followed again by a 360° rotation around the $\hat{j}$-*axis* which produces the following measurements:

$$\Psi_9 = K\,(m_x \cos\theta_{xj,k} + m_y \cos\theta_{yi,k} + m_z \cos\theta_{zk,k}),$$

$$\Psi_{10} = K\,(m_x \cos\theta_{xj,k} - m_y \cos\theta_{yk,k} + m_z \cos\theta_{zi,k}),$$

$$\Psi_{11} = K\,(m_x \cos\theta_{xj,k} - m_y \cos\theta_{yi,k} - m_z \cos\theta_{zk,k}),$$

$$\Psi_{12} = K\,(m_x \cos\theta_{xj,k} + m_y \cos\theta_{yk,k} - m_z \cos\theta_{zi,k}).$$

Finally, the magnetic moment components can be extrac[illegible] as

$$(\Psi_{1,3} + \Psi_{5,7})/4K = m_x \cos\theta_{xk,k} \cong m_x ,$$

$$(\Psi_{6,8} - \Psi_{2,4})/4K = m_y \cos\theta_{yk,k} \cong m_y ,$$

$$(2\Psi_{9,11} - \Psi_{1,3} + \Psi_{5,7})/4K = m_z \cos\theta_{zk,k} \cong m_z .$$

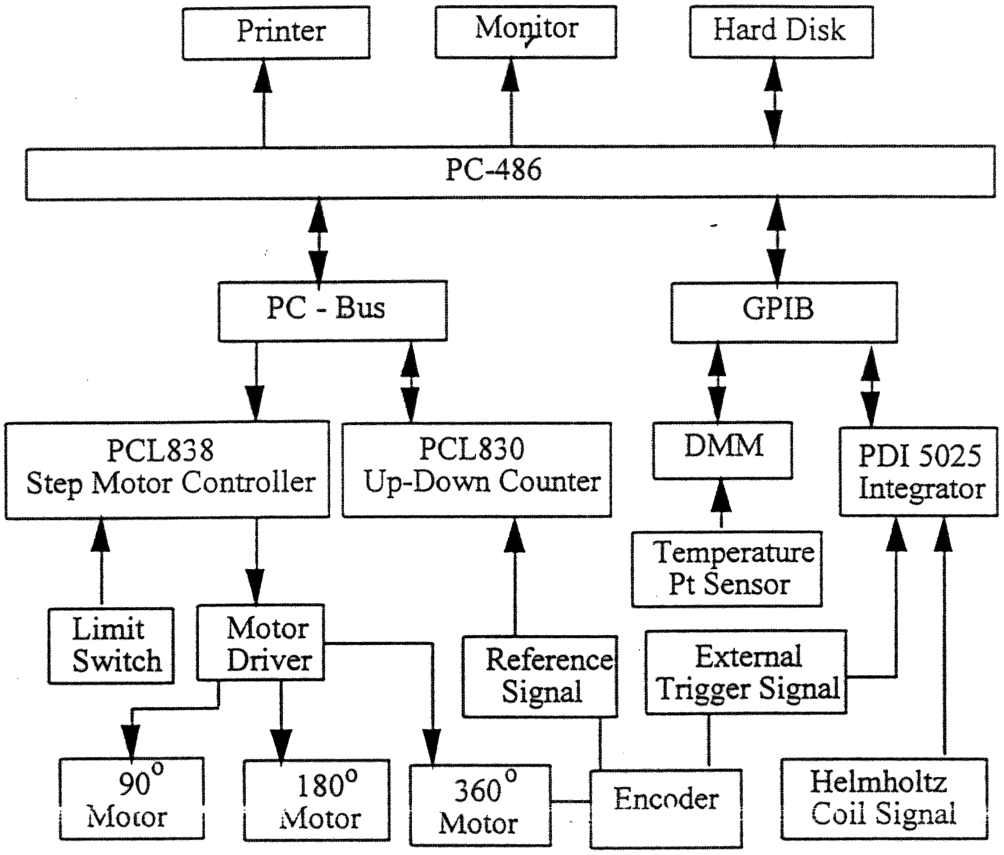

FIG. 3.12 The hardware architecture of the control system for the magnetic dipole moment measurement.

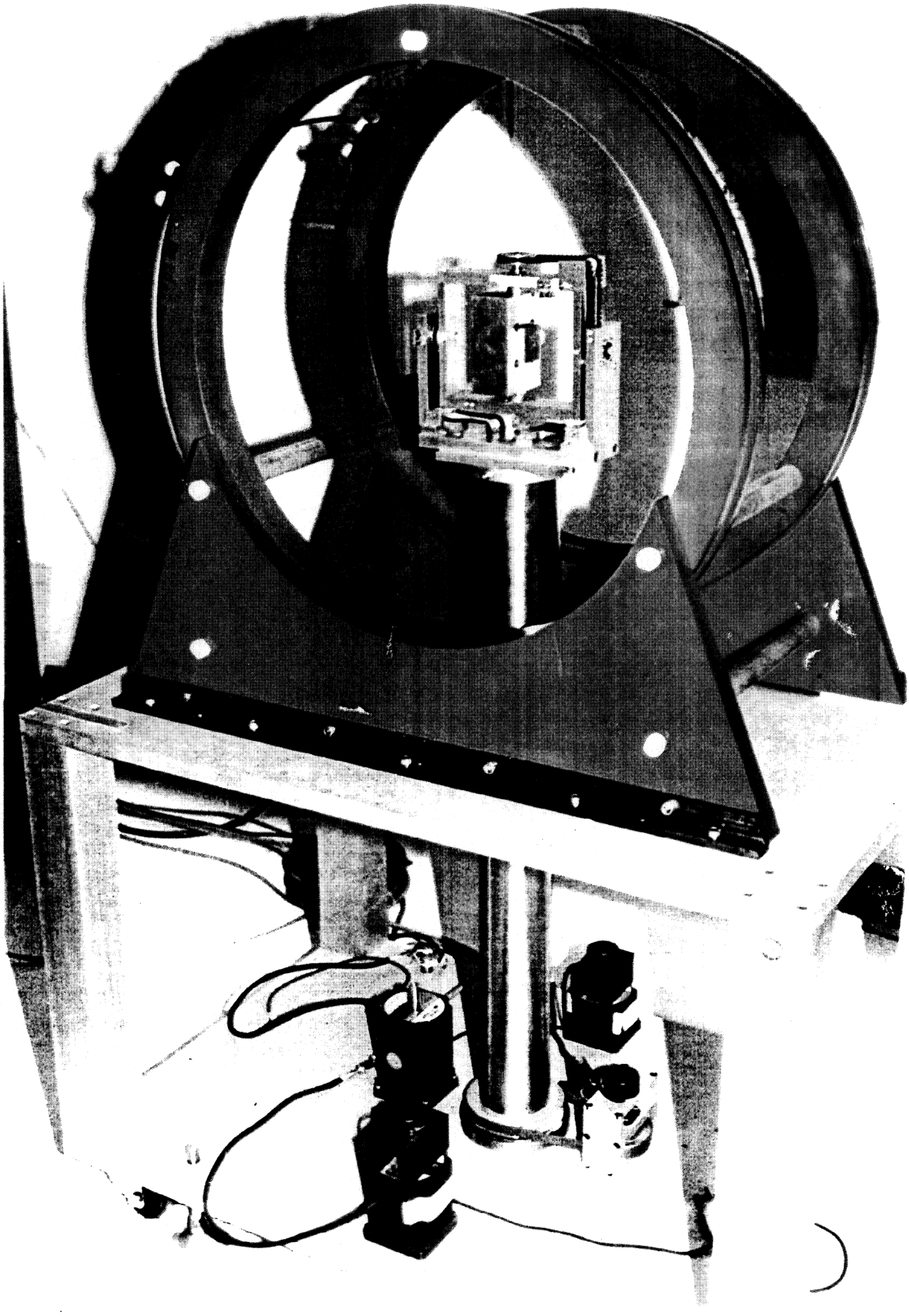

Component (Unit)	Block direction			
	$(\hat{x},\hat{y},\hat{z})$	$(\hat{-x},\hat{-y},\hat{z})$	$(\hat{x},\hat{-y},\hat{-z})$	$(\hat{-x},\hat{y},\hat{-z})$
m_z (T)	1.2273	1.2272	-1.2276	-1.2277
m_y (T)	0.0086	-0.0090	-0.0090	0.0087
m_x (T)	0.0139	-0.0135	0.0137	-0.0140

Replacing the different direction of the magnet on the holder to survey the absolute angle error and the main component deviation of the block magnetic moment of the measurement system. m_x , m_y and m_z is the average value on the each block direction.

① [illegible] for easy-axis

② 0.02° precision for two minor components

③ The system absolute accuracy is around 0.05°

④ The measurement speed is 4 blocks/h

Stretch-wire System for Integral Magnetic Field Measurements

First field integral measurement

$$I_y = \frac{\int Vdt}{N\Delta x}, I_x = \frac{\int Vdt}{N\Delta y}.$$

Second field integral measurement

$$II_y = -\frac{L}{2}\left[\frac{\int Vdt}{N\Delta x} + I_y\right], II_x = -\frac{L}{2}\left[\frac{\int Vdt}{N\Delta y} + I_x\right].$$

Harmonic field components measurement

$$\int_{t(\theta_i)}^{t(\theta_{i+1})} Vdt = N\int_{-\frac{L}{2}}^{\frac{L}{2}} dz \int_{\theta_i}^{\theta_{i+1}} B_r R d\theta .$$

$$\sum_{n=1}^{\infty} a_n cos(n\theta) + b_n sin(n\theta) = \sum_{n=1}^{\infty} \frac{2R^n N}{n}[A_n cos(n\theta) + B_n sin(n\theta)] sin\left(\frac{n\Delta\theta}{2}\right)$$

.

$$A_{n,j}^{skew} = \frac{r_{ref}^{n-j} A_n}{B_{ref,j}}, \quad B_{n,j}^{nor} = \frac{r_{ref}^{n-j} B_n}{B_{ref,j}}.$$

Stretch-wire System for Insertion Device Measurements

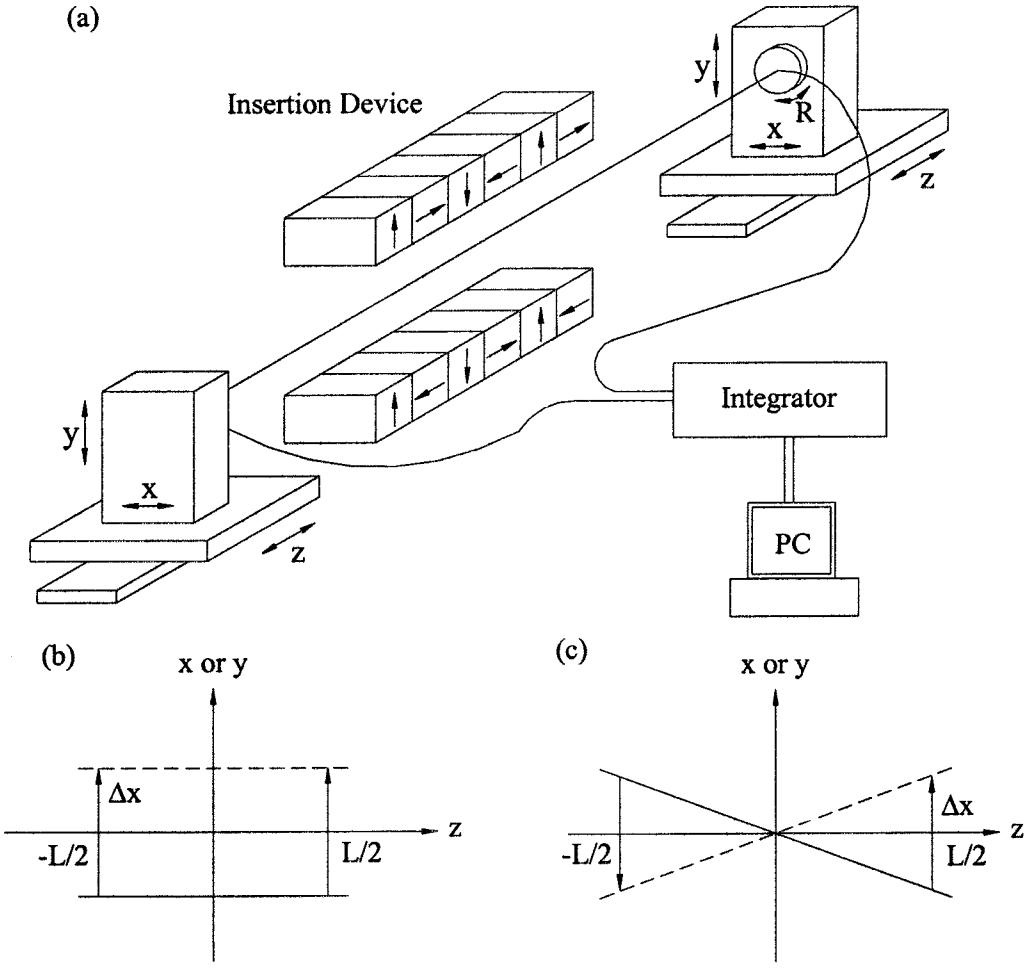

Stretch-wire System for Lattice Magnet Measurements

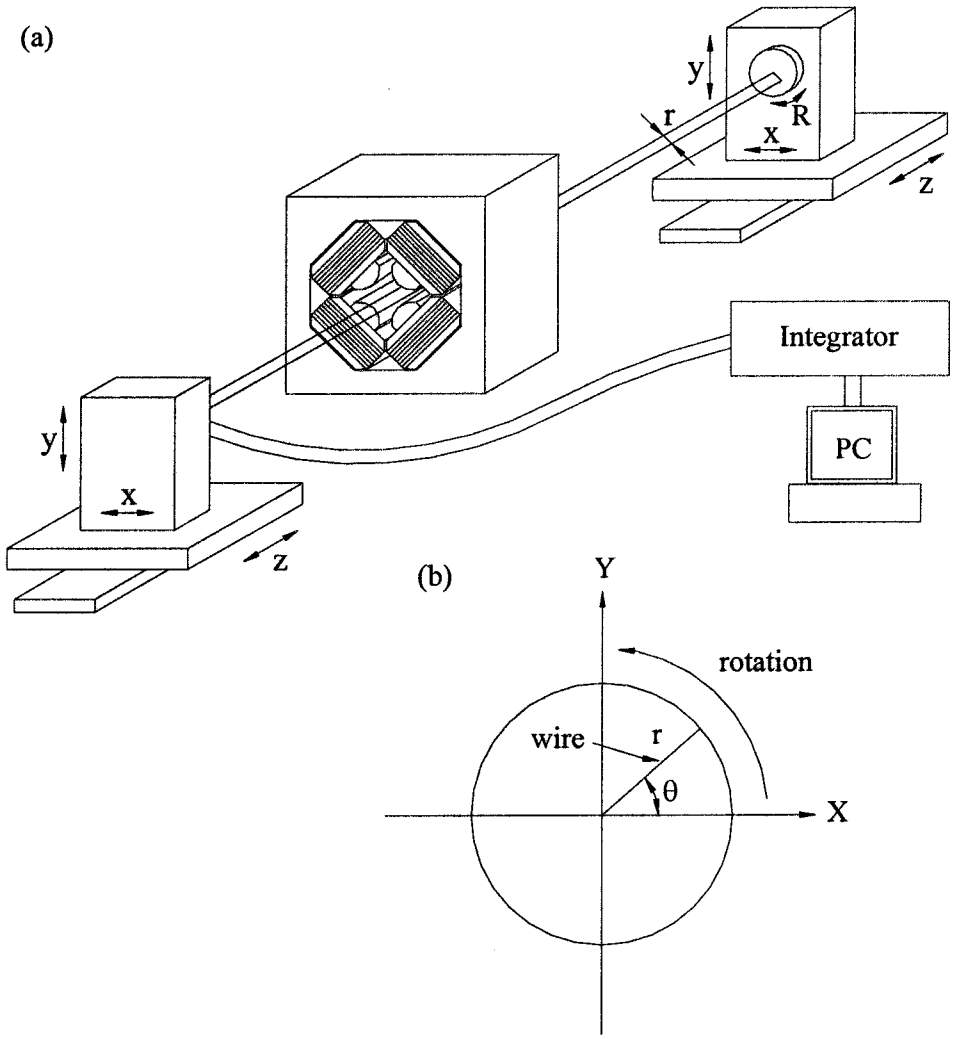

$$\delta = \frac{1}{2}\frac{\rho\vec{g}}{T} z(z-L)$$

For Cu-Be $$\delta = \frac{L^2}{8}\left(\frac{9.47\times10^{-3}\times1.1309\times10^{-4}\times9.8}{12000\times1.1309\times10^{-4}\times9.8}\right) \text{ cm}$$

$$= 0.987\times10^{-7} L^2 \text{ cm}$$

For Cu $$\delta = \frac{L^2}{8}\left(\frac{8.93\times10^{-3}\times1.1309\times10^{-4}\times9.8}{2500\times1.1309\times10^{-4}\times9.8}\right) \text{ cm}$$

$$= 4.465\times10^{-7} L^2 \text{ cm}$$

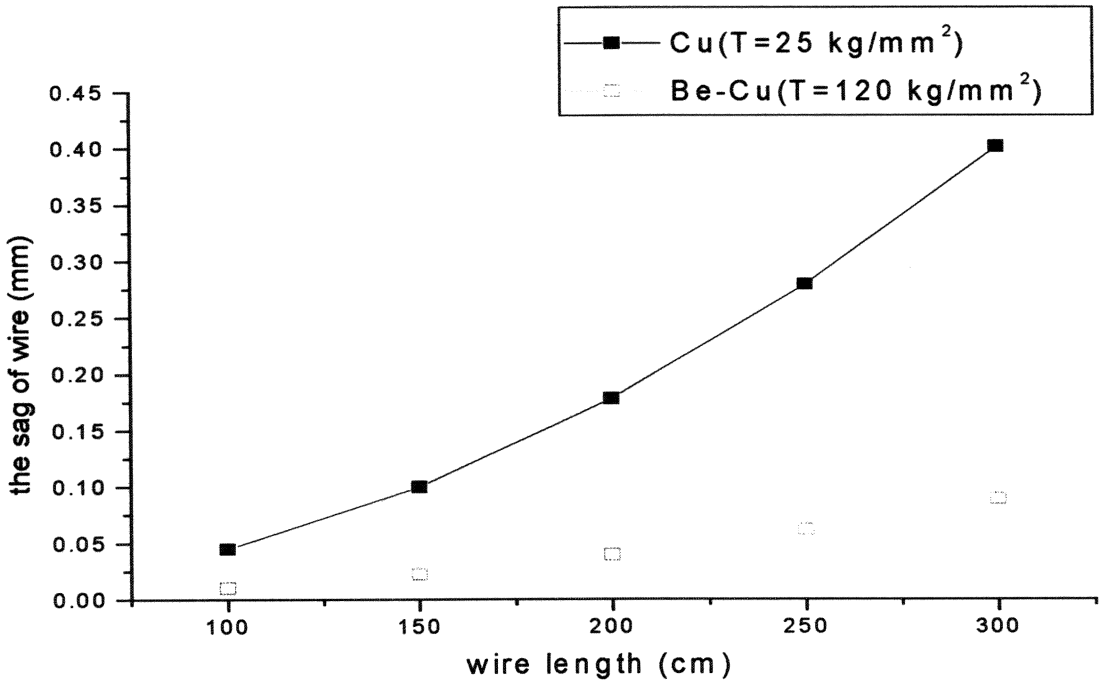

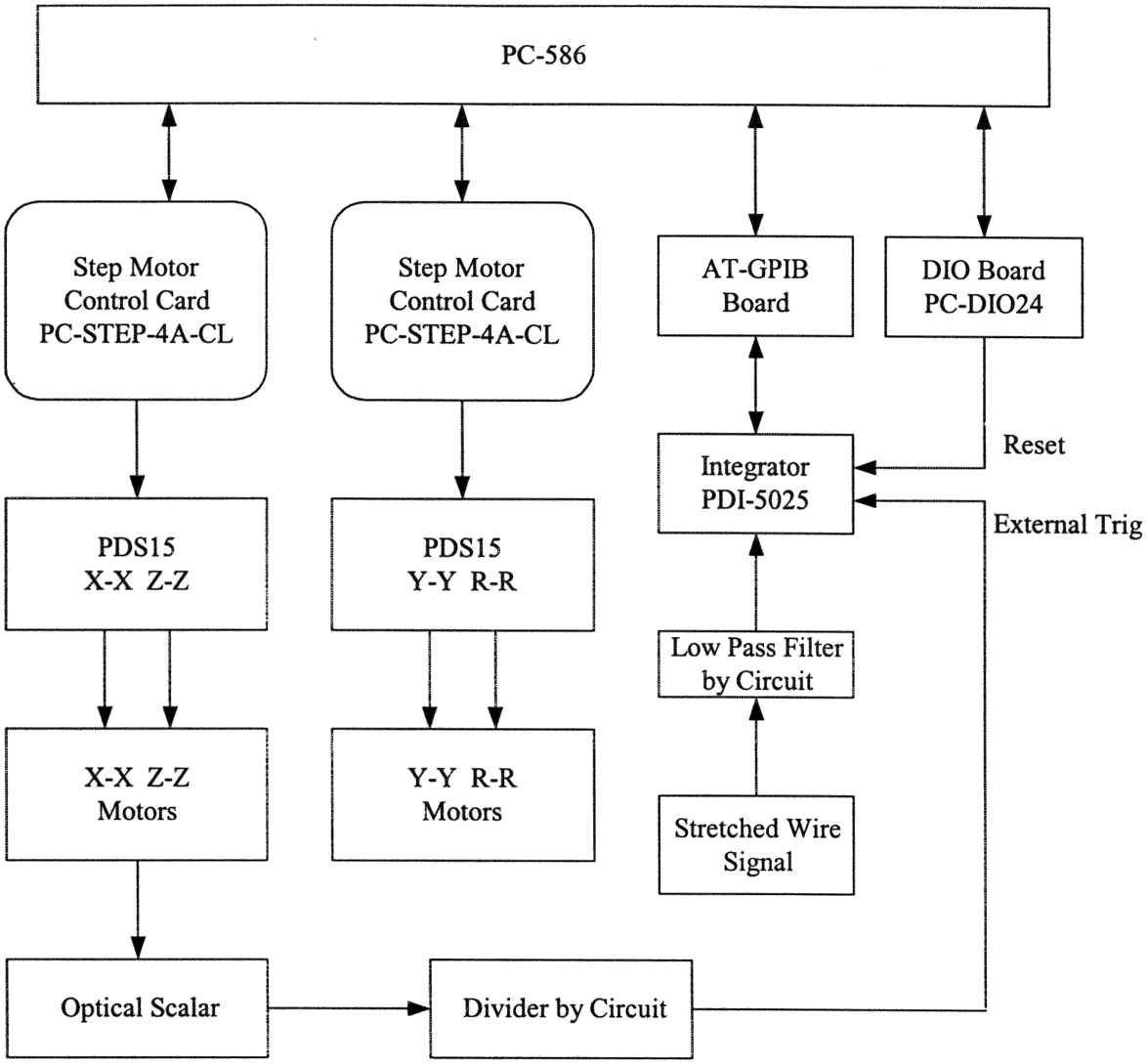
PC-586
Step Motor Control Card PC-STEP-4A-CL
Step Motor Control Card PC-STEP-4A-CL
AT-GPIB Board
DIO Board PC-DIO24
Reset
Integrator PDI-5025
External Trig
PDS15 X-X Z-Z
PDS15 Y-Y R-R
Low Pass Filter by Circuit
X-X Z-Z Motors
Y-Y R-R Motors
Stretched Wire Signal
Optical Scalar
Divider by Circuit

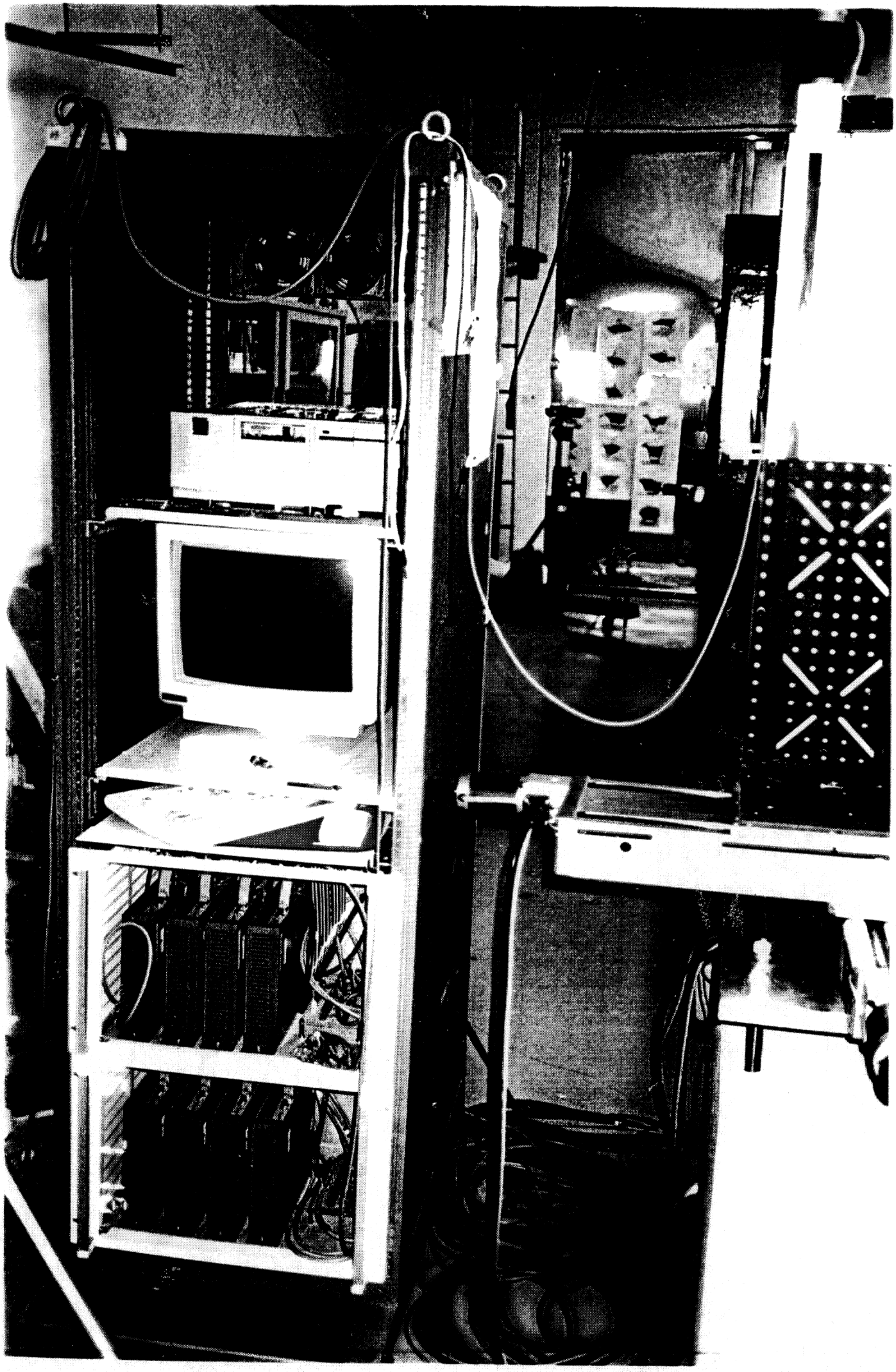

The measurement results of normalized harmonic field strength and the precision of dipole corrector, quadrupole, and sextupole magnet.

n	Dipole (%)	Quadrupole (%)	Sextupole (%)
1	100 ± 0.01	0.20 ± 0.02	1.27 ± 0.03
2	0.34 ± 0.01	100 ± 0.01	1.05 ± 0.04
3	0.52 ± 0.01	0.03 ± 0.01	100 ± 0.01
4	0.16 ± 0.02	0.04 ± 0.01	0.11 ± 0.01
5	0.24 ± 0.01	0.01 ± 0.01	0.10 ± 0.01
6	0.10 ± 0.01	0.56 ± 0.01	0.03 ± 0.01
9	0.06 ± 0.01	0.05 ± 0.01	0.12 ± 0.02
10	0.04 ± 0.01	0.23 ± 0.01	0.06 ± 0.01
14	0.04 ± 0.01	0.01 ± 0.01	0.05 ± 0.01
15	0.05 ± 0.01	0.01 ± 0.01	0.06 ± 0.02

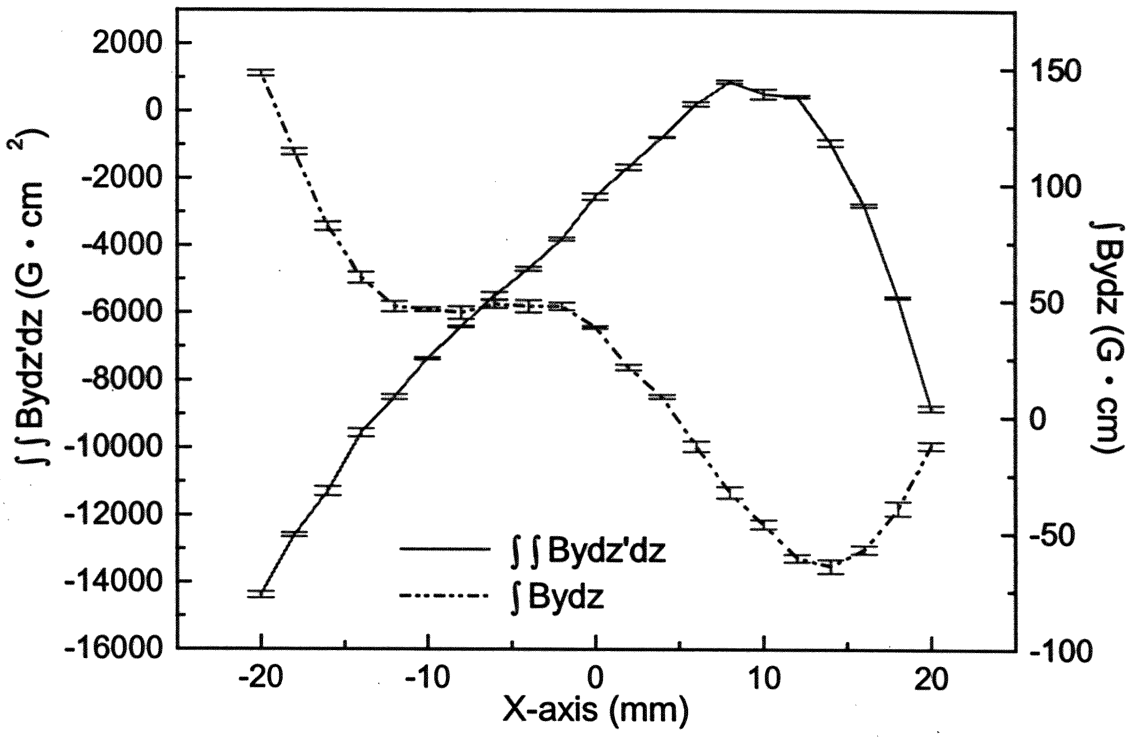
2000
0
-2000
-4000
-6000
-8000
-10000
-12000
-14000
-16000
∫∫Bydz'dz (G • cm 2)
150
100
50
0
-50
-100
∫Bydz (G • cm)
-20
-10
0
10
20
X-axis (mm)
∫∫Bydz'dz
∫Bydz

Stretch wire measurement system

❖ Advantage:

- **A simple mechanical structure with reliable high precision**
- **Easy to exchange the measurement method and easy operation**
- **It can be for first and second field integral measurement on insertion device and for harmonic field measurement on lattice magnets**

❖ Crucial issue:

- **Electronic drift and gain in linearity of the integrator should be improved**
- **The inexact coupling between the coupler and the rotor should be reduced**
- **The deviation of wire rotating center and the sag of wire should be avoided**
- **The wire length for the harmonic components measurement should be within 1 m long for Cu wire and 2.5 m long for Be-Cu wire to keep high precision of 0.01%**
- **Use the Litz wire to enhance the resolution and accuracy**

Simple rotating coil measurement system

❖Relative issue discussion:

- **PDI 5025 integrator with 32 bit counters to solve the resolution and the rotation speed variation**
- **High precision angular encoder with 1000 angle to avoid the time integration error and to increase resolution**
- **Transmission mechanism of the shaft coupling between the encoder and the rotating cylinder should be a precision align**
- **The position reproducibility is not easy to be solved of the conical taper rings, the position reproducibility is 0.15 mm**
- **A precise mass symmetry on the rotating cylinder is very important to avoid the sag of rotating coil which was fixed on rotating cylinder**

3D-Hall probes on the fly mapping method

❖ Advantages and disadvantage:

- Perform the point and integral field measurement for *only the straight magnets*
- provide the criterion for the fast shimming of the photon spectrum, multipole components, electron trajectory of insertion devices
- time consuming but the Measurement speed is much faster than the "on static" fixed angle Hall probe method.
- *Real field measurement* of three magnetic field components without any field correction.

❖ Critical issues

- **Position calibration on a reference magnet should be very careful**
- **The planar Hall effect should be considered**
- **Field calibration should consider the orthogonal between the three Hall probe on the exact angle**

91 7 96

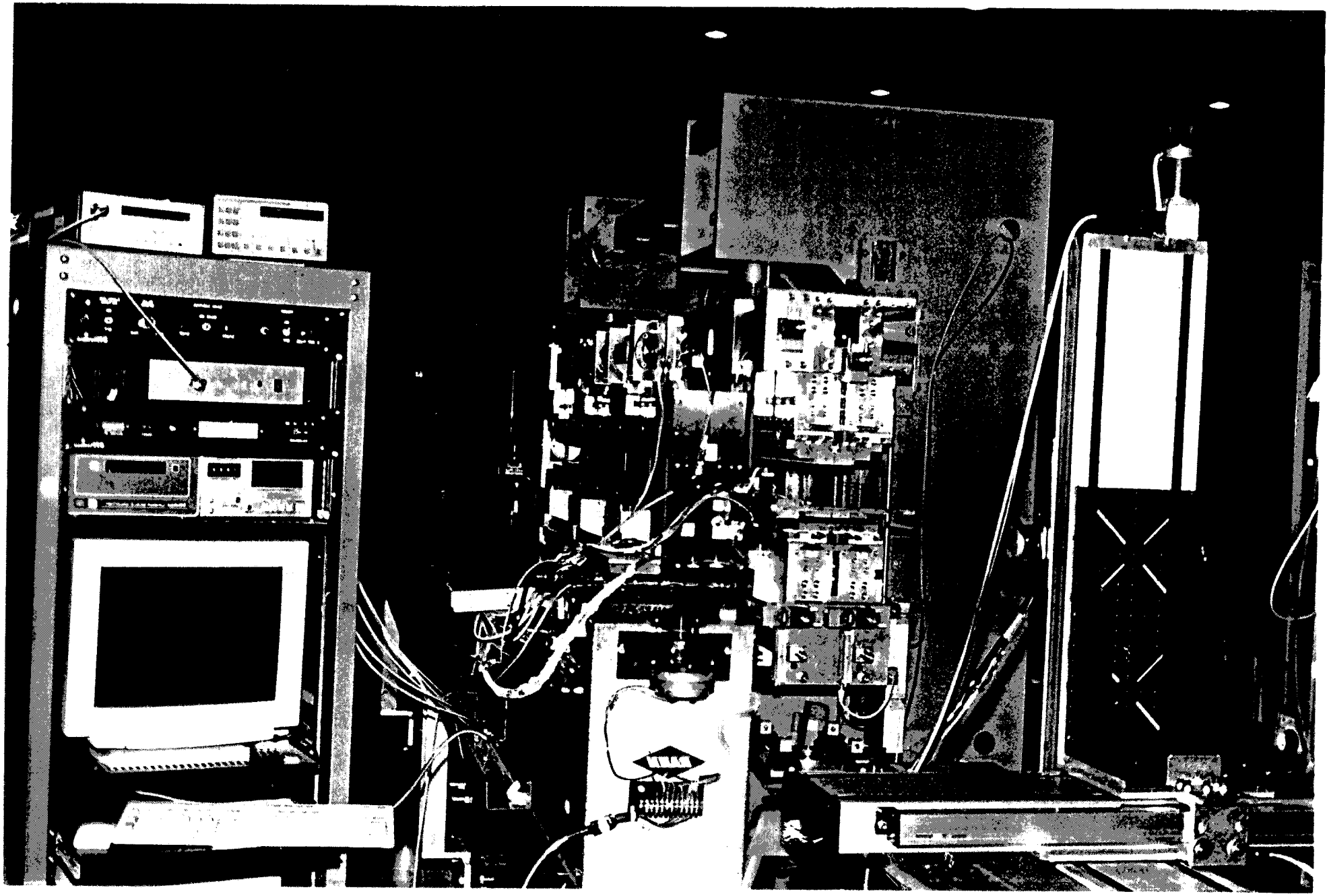

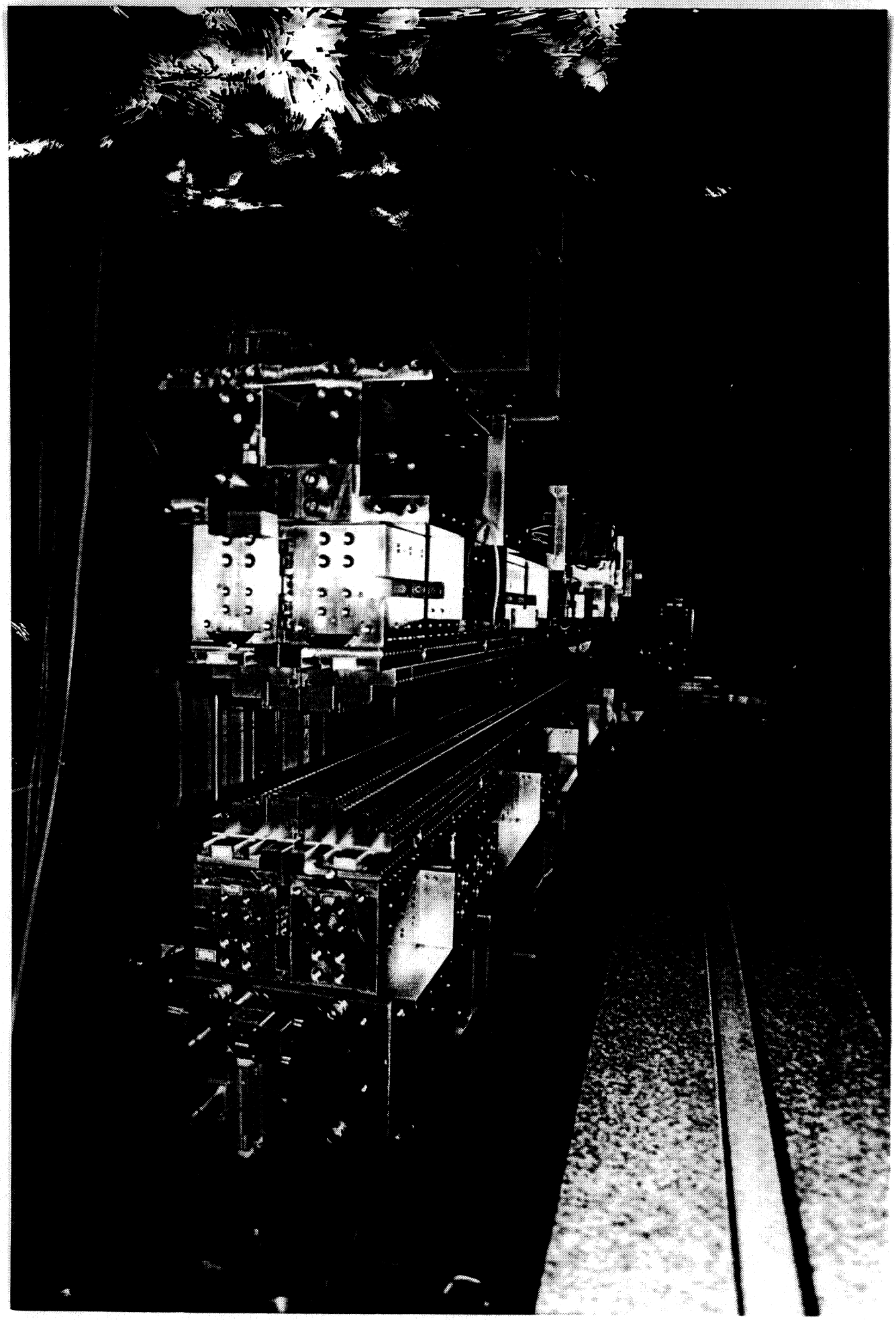

(a)

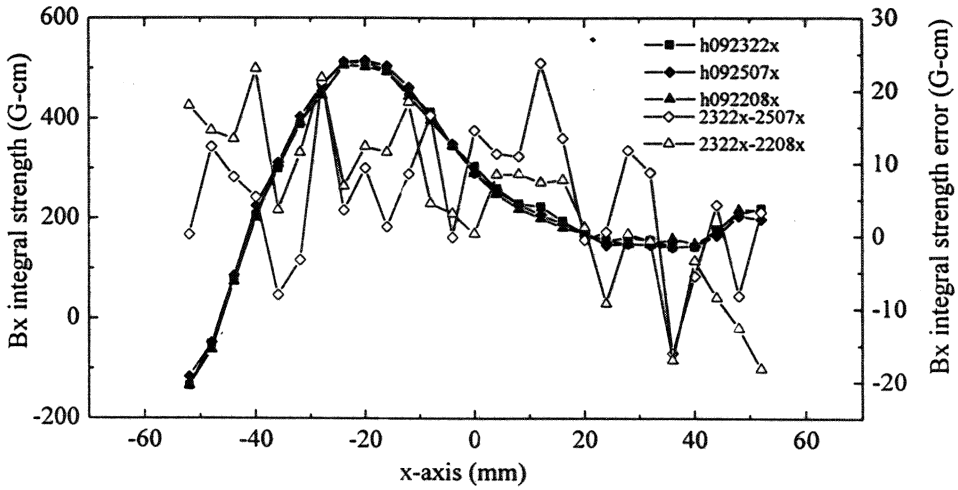
h092322x
h092507x
h092208x
2322x-2507x
2322x-2208x
Bx integral strength (G-cm)
Bx integral strength error (G-cm)
x-axis (mm)

(b)

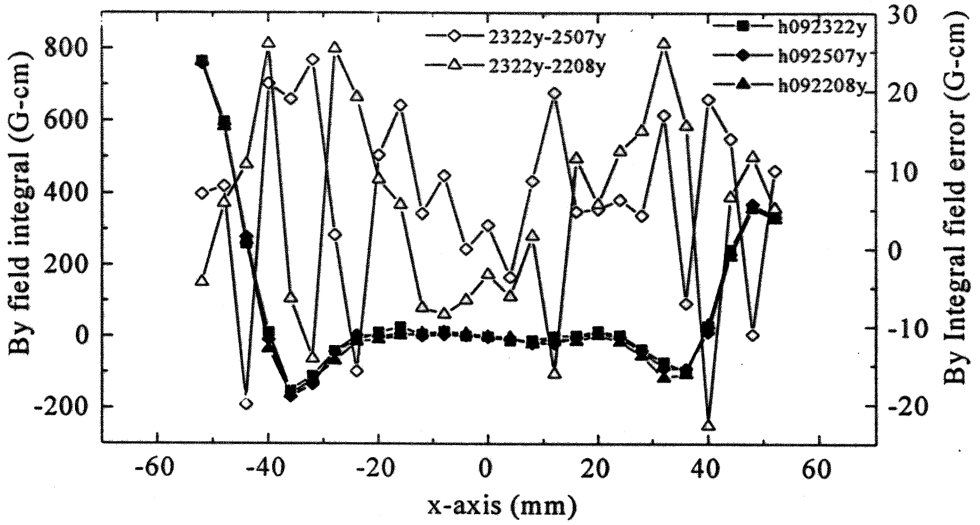
2322y-2507y
2322y-2208y
h092322y
h092507y
h092208y
By field integral (G-cm)
By Integral field error (G-cm)
x-axis (mm)

(c)

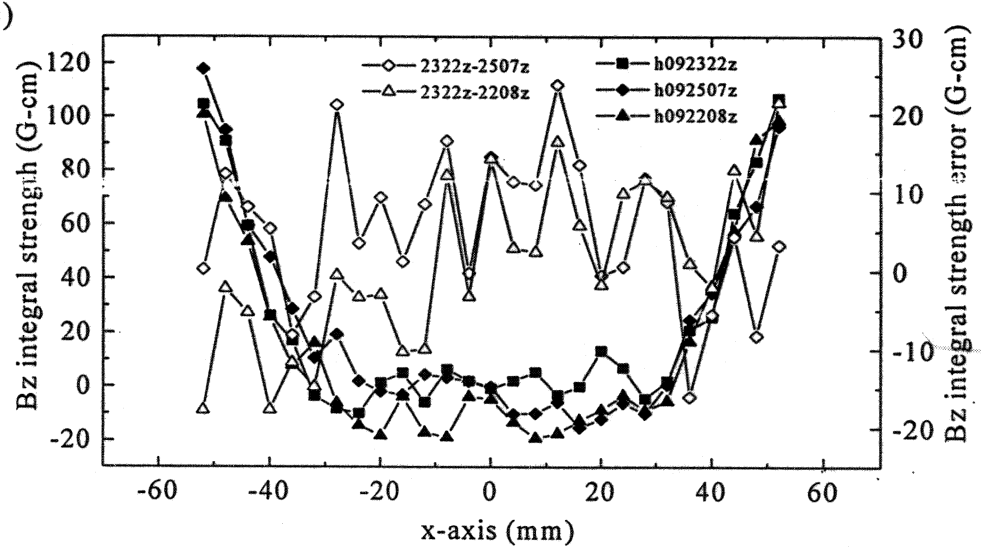
2322z-2507z
2322z-2208z
h092322z
h092507z
h092208z
Bz integral strength (G-cm)
Bz integral strength error (G-cm)
x-axis (mm)

Simple rotating coil system method

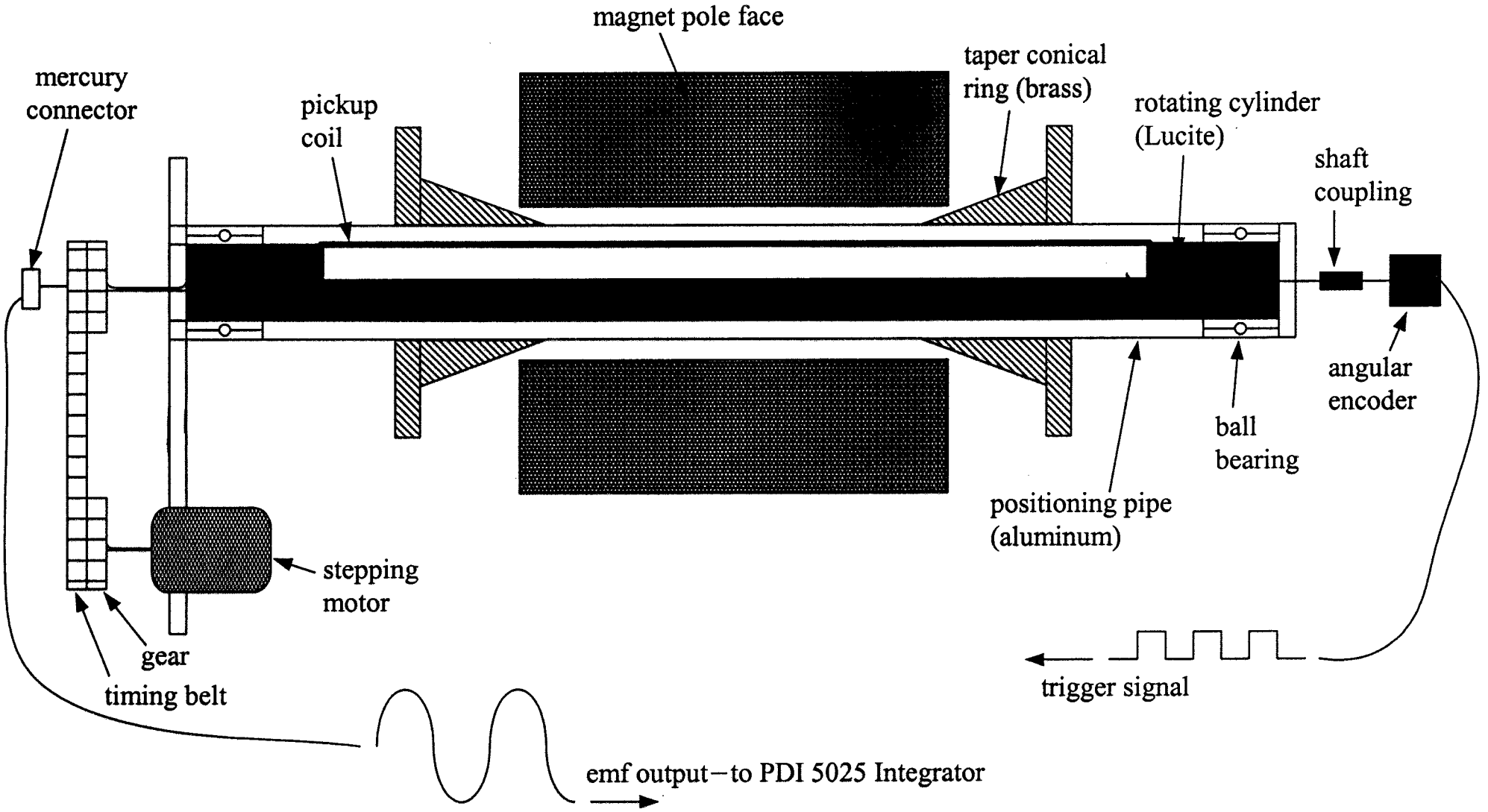

Simple rotating coil measurement system

❖Advantage:

- It was a simple structure
- Easy to operate
- Inexpensive
- Self centering rotating coil

❖Disadvantage:

- Low precision of alignment (alignment error 0.15 mm)
- Precision of the harmonic components below $1x10^{-4}$ due to the alignment error
- Easy to create the error of the accuracy & precision
- Short term stability due to the coil sag

Pulse Wire Method

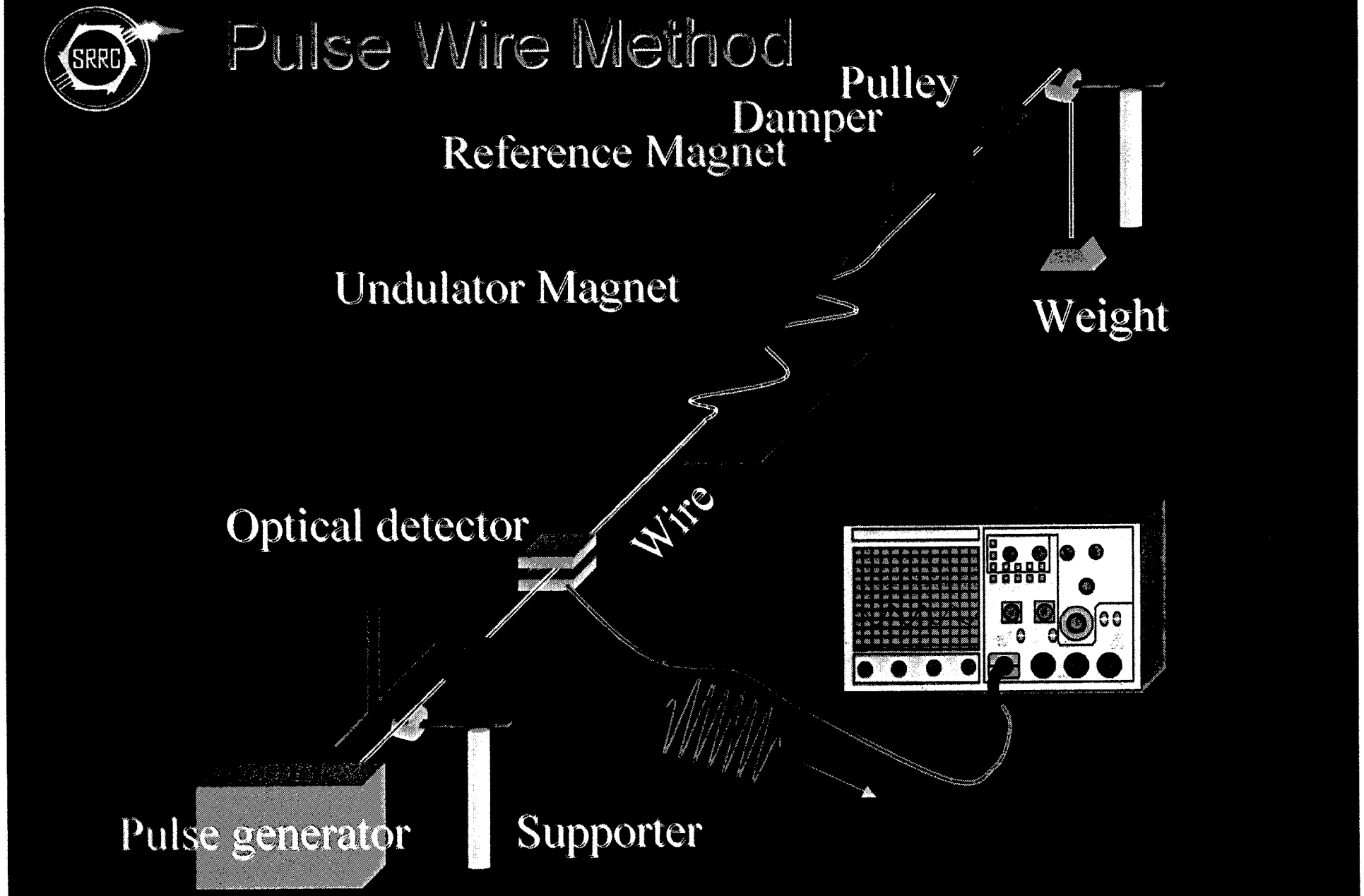

The spurious components occurred while using thin wire

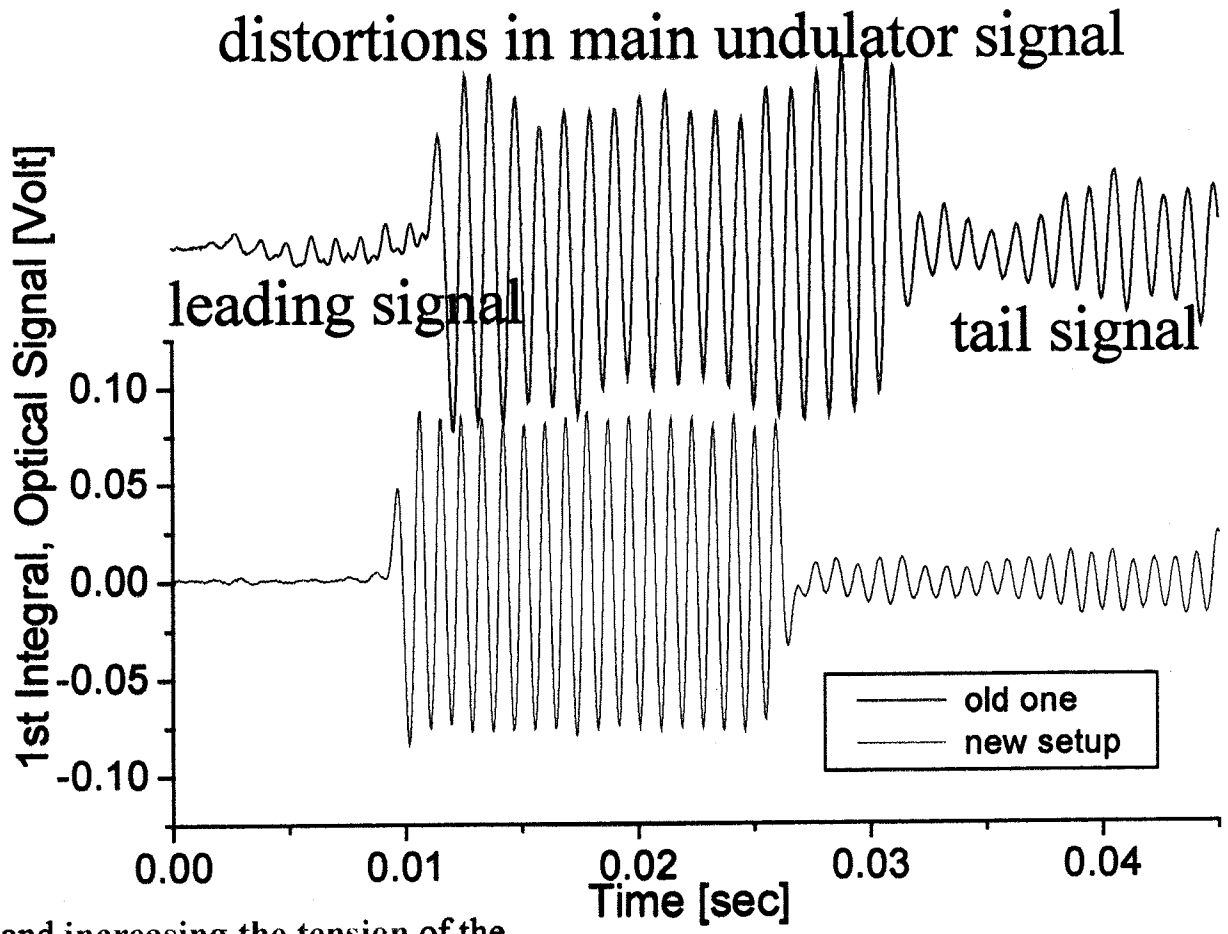

After readjustment and increasing the tension of the wire, one can eliminate some leading signal and get the lower curve.

A simulation of imperfection effect on tail signal with imperfections putting at the different position.

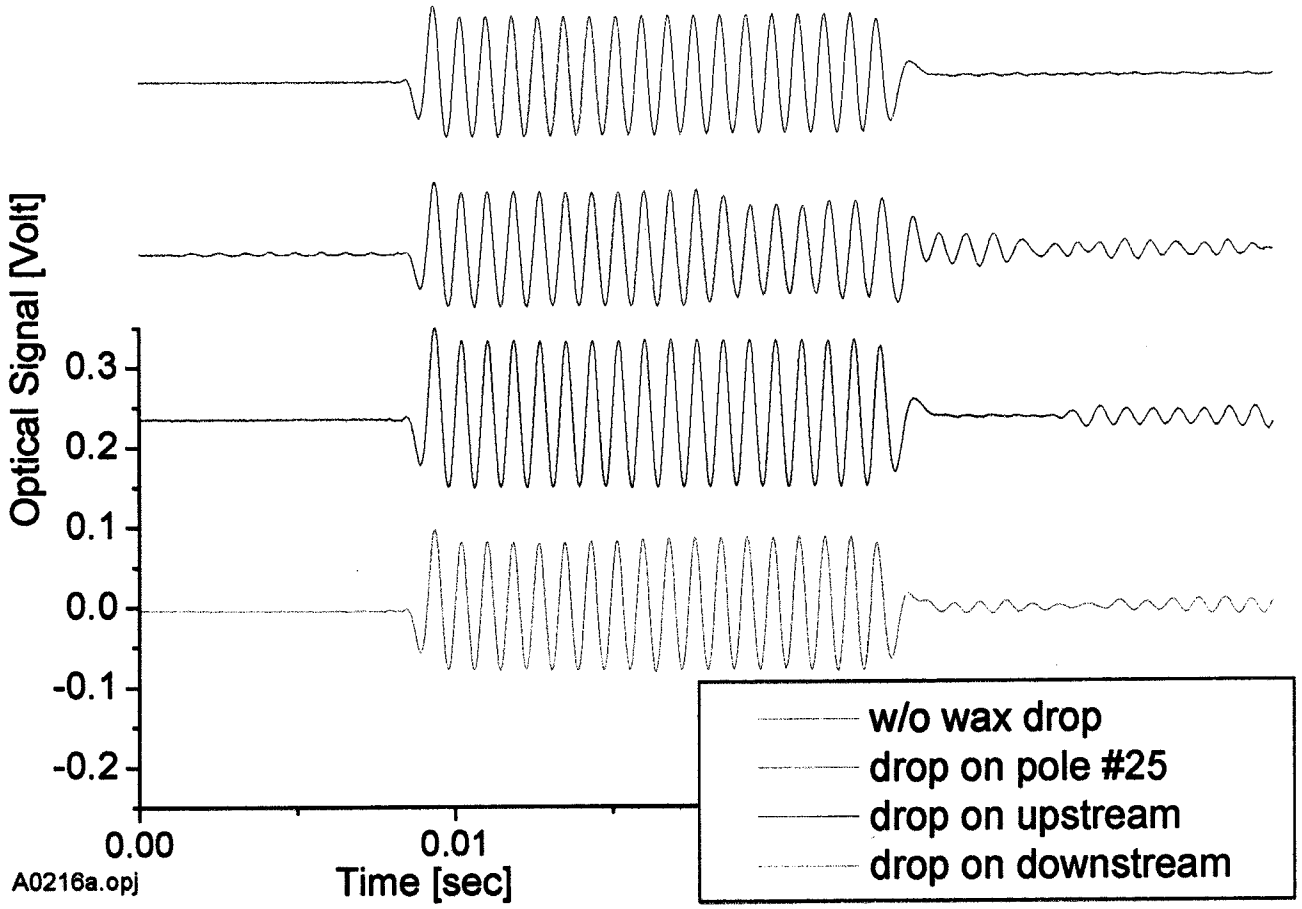

If this imperfection hypothesis is accepted, one can expect that a thick wire would not be sensitive to the impurity of the wire and have a better uniformity and less tail signal.

We replace the wire with 125 μm diameter by a 250 μm one and indeed can reduce the signal.

A comparison between thick pulse wire without trace back compensation and Hall probe measurement

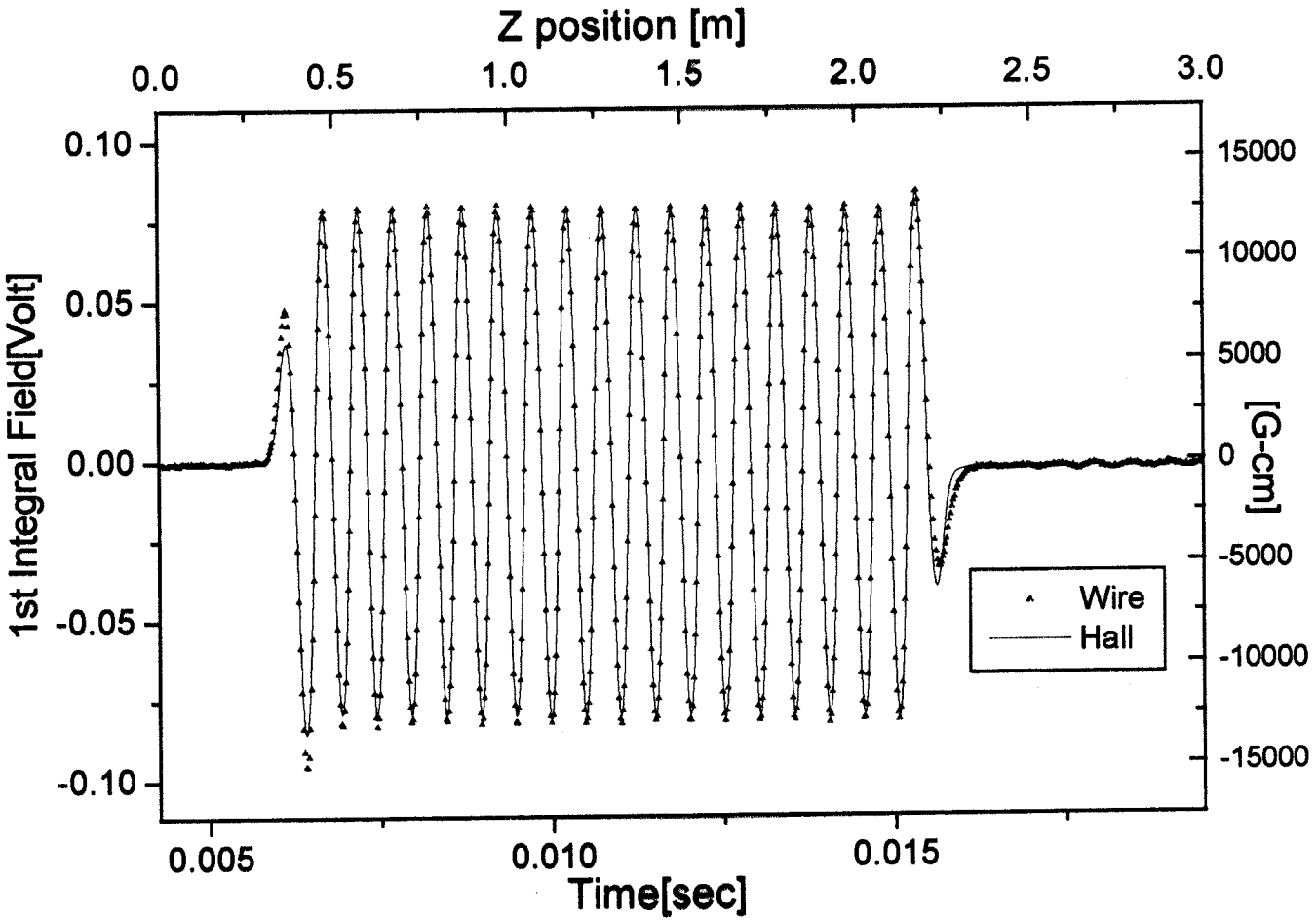

The observation of wave distortion at different distances from the same source excited by a reference magnet

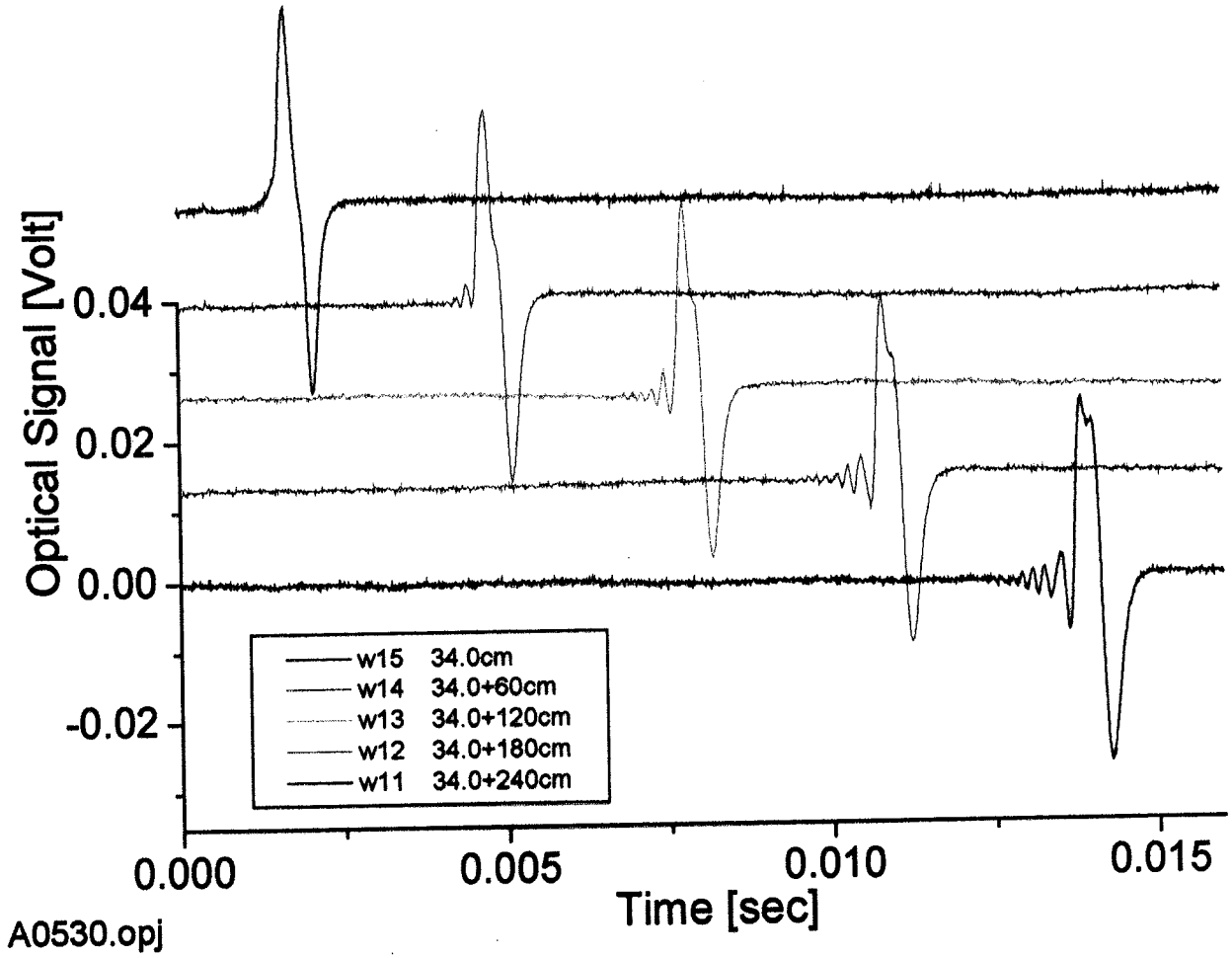

The transverse-motion equation is first derived by Lord Rayleigh

$$-EI\frac{\partial^4 x}{\partial z^4}+T\frac{\partial^2 x}{\partial z^2}=\rho A\frac{\partial^2 x}{\partial t^2}$$

I: moment of inertia
A: cross section
E : modulus of elasticity
ρ: mass density
T: tension

By considering the solution

$$x=Ce^{i(kz-\omega t)}$$

gives dispersion function

$$k(\omega)=\pm\sqrt{\frac{T}{2EI}}\sqrt{-1\pm\sqrt{1+4\frac{\rho AEI}{T^2}\omega^2}}$$

A comparison between trace-back thick pulse wire calculation and Hall probe measurement

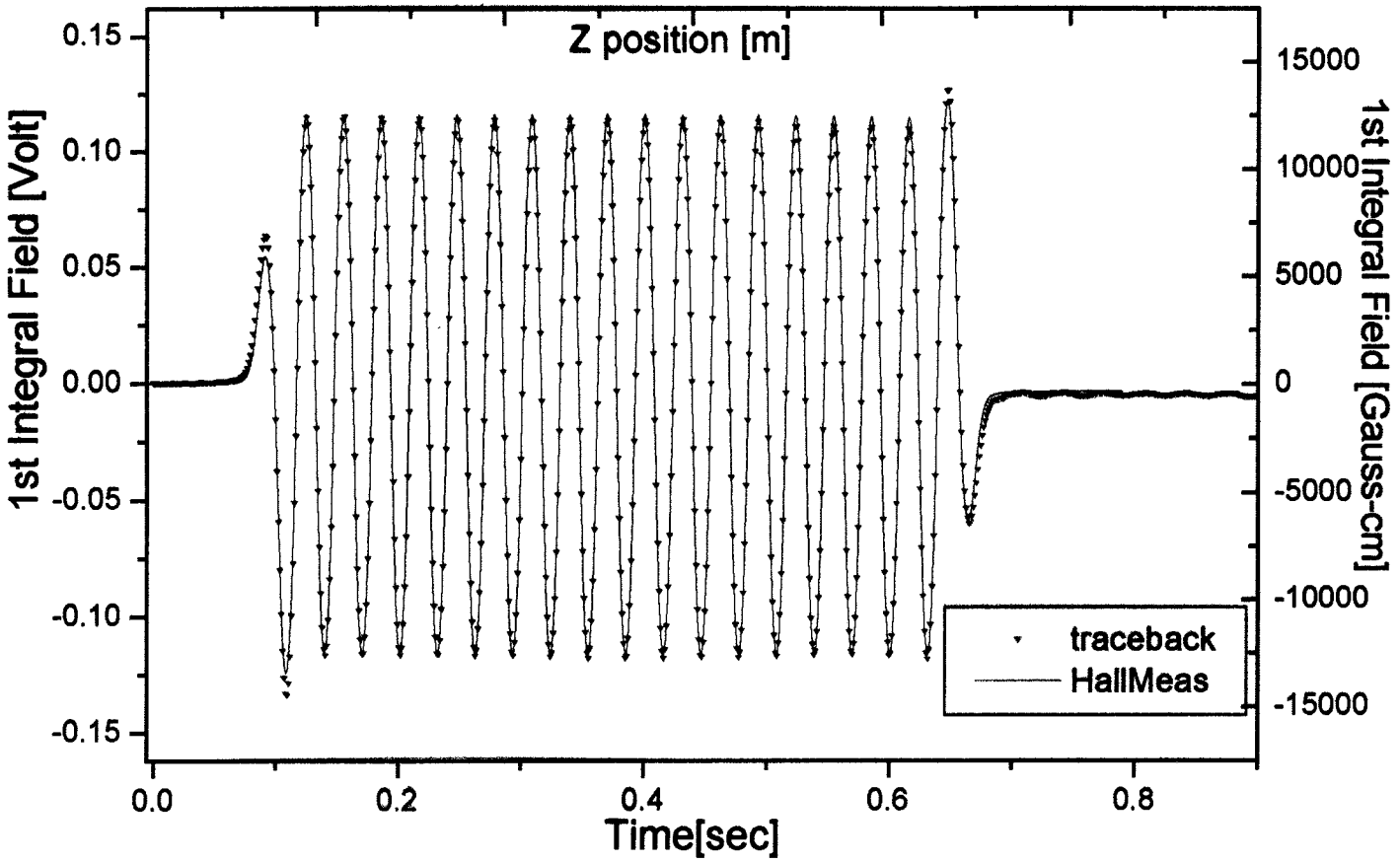

Pulse wire method

❖ **Advantages and critical issues:**

- **Make *in situ measurement* of wiggler magnetic field so as to monitor the field error and cancel the wiggler steering errors**
- **In the point measurement of *mini-gap undulator***
- **To measure the *dynamic behavior* of the Pulsed magnets and current ramping of wiggler**
- **To *speed the fine-tuning* of wiggler field**
- **The wire imperfection from uniformity or impurity will create the wave distortion - improvement by thick wire**
- **The dispersion of acoustic wave due to the phase variation can be reduced by increase the wire tension**
- **Using the FFT and inverse FFT to perform the trace back procedure in order to compensate the dispersive wave**